MODELLING FLUXES AND CONCENTRATIONS OF CO_2, H_2O AND SENSIBLE HEAT WITHIN AND ABOVE A MOUNTAIN MEADOW CANOPY: A COMPARISON OF THREE LAGRANGIAN MODELS AND THREE PARAMETERISATION OPTIONS FOR THE LAGRANGIAN TIME SCALE

GEORG WOHLFAHRT[*]

Institut für Botanik, Universität Innsbruck, Sternwartestr. 15, 6020 Innsbruck, Austria

Abstract. Two simple analytical Lagrangian and a Lagrangian random walk model, together with three options for the parameterisation of the Lagrangian time scale, are compared in their ability to predict fluxes and scalar concentrations of CO_2, H_2O and sensible heat within and above a mountain meadow in the eastern Alps. Results indicate that both scalar concentrations and ecosystem fluxes exhibit little sensitivity to the differences between the investigated models and may be predicted satisfactorily by one of the simpler models so long as the source/sink strength is parameterised correctly. Model results also show little sensitivity to the parameterisation of the vertical variation of the Lagrangian time scale, yet the increase of the Lagrangian time scale towards the ground predicted by one of the three investigated parameterisation options resulted in less agreement with measurements as compared to the other two, which assumed the Lagrangian time scale to be either constant with height or to decay towards zero at the ground surface. Correspondence between simulated and measured fluxes and scalar concentrations of CO_2, H_2O and sensible heat were generally satisfactory, except for shortly after the meadow was cut, when the significant increase of respiratory carbon losses could not be captured by the model.

Keywords: Evapotranspiration, Grassland, Localised near-field theory, Photosynthesis, Respiration, SVAT model, Turbulent dispersion.

1. Introduction

The implicit problem of deducing both the vegetative source/sink strength and scalar concentrations when they are linked by a specified relationship (Raupach et al., 1997), continues to be a subject of active discussion within the terrestrial branch of the biosphere-atmosphere modelling community. Early K-theory models (Goudriaan, 1977) were based on the idea that turbulence within the plant canopy behaves entirely diffusively, scalar material accordingly being transported down concentration gradients proportional to a so-called eddy diffusivity. While the theoretical deficiencies of these models are now commonly acknowledged, they are still in use and comparisons with more complex models suggest that K-theory is adequate for predicting scalar concentrations and fluxes under many circumstances

(Dolman and Wallace, 1991; Van den Hurk and McNaughton, 1995; McNaughton and Van den Hurk, 1995; Wilson et al., 2003). Lagrangian random walk models are able to account for the effects of persistence of turbulent dispersion in the vicinity of sources/sinks where K-theory fails (Raupach, 1987, 1988), but are much more complex and computationally demanding. Motivated by the demand for a physically realistic, yet simple and computationally efficient (analytical), model Raupach (1989a, b) developed the so-called localised near-field (LNF) theory. The LNF theory employs Lagrangian principles to decompose the scalar concentration field into a near-field part, where transport is dominated by the persistence of turbulent motions, and a far-field part, where transport is essentially diffusive. Several applications of the LNF theory, albeit mainly in its inverse form (Katul et al., 1997; Denmead et al., 2000; Harper et al., 2000; Leuning et al., 2000; Ogee et al., 2003), have shown that it provides a reasonable approximation of within-canopy turbulence. Recently, Warland and Thurtell (2000) improved upon this concept and introduced what they called a 'mixing matrix' model. The most significant difference to the LNF theory is that their model describes dispersion from the near- to far-field continuously and uses turbulence statistics at all heights in both near- and far-field calculations. As shown by the same authors for an artificial canopy with a known heat source strength, these improvements result in better correspondence with measured air temperatures close to the heat source as compared to the LNF theory. Yet up to now, except for Wilson et al. (2003), their model has not been tested under field conditions. For the implicit problem also, there exist few comparisons between simple analytical and Lagrangian random walk models, in particular for field conditions.

The first aim of the present paper is thus to assess how complex turbulent dispersion models need to be in order to successfully predict scalar concentrations and fluxes within and above the plant canopy, and whether simple analytical models may serve as substitutes for random walk models. To this end the performance of the LNF theory (Raupach, 1989a, b) and the 'mixing matrix' model (Warland and Thurtell, 2000) is compared to the Lagrangian random walk model of Baldocchi (1992). No attempt will be made to assess the performance of K-theory models, (i) because their limitations are well-known, and (ii) because with regard to computational efficiency, differences between K-theory and analytical Lagrangian models are anyhow likely to be small, and (iii) because such comparisons have already been conducted in the past (see references cited above).

Lagrangian dispersion models (for one-dimensional applications) require the vertical variation of turbulence statistics, i.e., the vertical velocity standard deviation (σ_w) and the Lagrangian time scale (T_L), to be specified: σ_w may be directly measured or alternatively simulated with reasonable success based on second- or higher-order closure models (Massman and Weil, 1999; Lai et al., 2000a, b). In contrast, the specification of T_L remains somewhat speculative, since it cannot be measured directly, but is usually inferred by applying Taylor's frozen-turbulence hypothesis to single-point measurements of its Eulerian counterpart, T_E,

as $T_L = \beta u\, T_E/\sigma_w$, where u is the mean streamwise wind speed and β is a constant of order 1 (Raupach, 1989b). Given the uncertainties inherent to this approach (Raupach et al., 1996), it is not particularly surprising that the parameterisations of T_L found in the literature differ widely, both with regard to the vertical variation, as well as the absolute magnitude. The mixing-layer analogy (Raupach et al., 1996) provides a quantitative means to incorporate the effects of canopy structure into the estimation of the absolute values of T_L in the upper canopy region, but the vertical variation of T_L, particularly in the lower canopy layers, remains essentially hypothetical: Raupach (1988) assumed T_L to be constant with height, Leuning et al. (2000) assumed T_L to decay to zero in the lower quarter of the canopy, whereas the second-order closure model of Massman and Weil (1999) predicts T_L to increase towards the ground.

The second aim of the present paper is thus to combine the comparison of the three Lagrangian models mentioned above, with a comparison of these three contrasting parameterisations of T_L.

The ability of the investigated model/parameterisation combinations to predict scalar concentrations and fluxes of CO_2, H_2O and sensible heat will be tested for a mountain meadow in the Stubai Valley, a valley typical for the Austrian part of the eastern Alps. The various combinations of turbulent dispersion models and parameterisations of T_L are incorporated into a one-dimensional soil-vegetation-atmosphere-transfer (SVAT) model developed with special emphasis on multi-species mountain grassland ecosystems (Wohlfahrt et al., 1998, 2000, 2001; Wohlfahrt and Cernusca, 2002). In order to be able to study the effects of canopy development (i.e., the changes in plant area density and canopy height) on model predictions, the time period between the first and second cut, during which the plant area index increases more than threefold, was selected for the present study. Model performance is assessed by comparison with scalar concentration and eco-system flux measurements conducted throughout this period. The parameterisation of the vegetative (and soil) source/sink strength is based on eco-physiological, plant ecological and micrometeorological measurements carried out at this site since 1999.

2. Material and Methods

2.1. SITE DESCRIPTION

Investigations were carried out at a meadow in the vicinity of the village Neustift (47°07′ N, 11°19′ E) in the Stubai Valley (Austria), as a part of a larger programme aimed at quantifying the effects of land-use changes on the carbon cycle of mountain grassland ecosystems. The study site is situated at an elevation of 970 m a.s.l. in the middle of the flat valley bottom. The fetch is homogenous up to 300 m to the east and 900 m to the west of the instrument tower, the dominant day and

night time wind directions, respectively. The average annual temperature is 6.3 °C, and average annual precipitation amounts to 850 mm. The snow-free (vegetation) period usually extends from mid March to mid November. The meadow is cut twice a year, during year 2001 on day-of-year (DOY) 171 and 226, the intermediate period was selected for the present study.

The vegetation has been classified as a Pastinaco-Arrhenatheretum and consists mainly of a few dominant graminoid (*Dactylis glomerata*, *Festuca pratensis*,*Phleum pratensis Trisetum flavescens*) and forb (*Ranunculus acris*, *Taraxaxum officinale*, *Trifolium repens*, *Trifolium pratense*, *Carum carvi*) species. The soil has been classified as a Fluvisol (FAO classification) and is approximately 1 m deep. Below a thin (0.001 m) organic layer, an A horizon, with an organic volume fraction of approx. 14%, extends down to 0.02 m, followed by the B horizon, which is best described as a (sandy) loam. Roots reach down to 0.5 m, but 80% of them are concentrated in the upper 0.13 m of the soil.

2.2. EXPERIMENTAL METHODS

Canopy structure was assessed in a destructive fashion by stratified clipping (Monsi and Saeki, 1953) of square plots of 0.25 m^2 at DOYs 172, 198 and 225, i.e., immediately after the first cut, halfway between the first and second cut, and immediately before the second cut. Thickness of the harvested layers ranged between 0.05 and 0.1 m, depending on plant area density. The harvested plant material was separated according to combined functional and taxonomical criteria: leaves were separated into those species that had the largest fractional contribution to the total plant area index (PAI m^2 plant area per m^2 ground area), i.e., *Ranunculus acris*, *Taraxaxum officinale*, *Trifolium repens*, *Trifolium pratense*, *Carum carvi*. The remaining leaves, as well as all stems, were pooled to two functional groups, namely remaining forbs and graminoids. The remaining plant components, i.e. reproductive organs, attached dead plant matter and cryptogams, were pooled over all species. Silhouette plant areas were determined by the means of an area meter (LI-3100, Li-Cor, Lincoln, U.S.A.). After oven drying at 70 °C for at least 72 hrs, the plant material was weighed (AE-260, Mettler Instrumente AG, Greifensee-Zürich, CH), ground and analysed for total nitrogen using an elemental analyser (CHNS-932, LECO Instruments, St. Joseph, U.S.A.). Phytoelement inclinations and widths were measured in the field with a hand inclinometer with five degrees accuracy and a ruler, respectively.

Leaf gas exchange measurements and the subsequent parameterisation of respective leaf gas exchange models were carried out on the forb species mentioned above and the graminoid *Dactylis glomerata*, as described previously in detail by Wohlfahrt et al. (1998, 1999), and are thus not repeated. The corresponding model theory and parameters are given in Appendix A.

Net ecosystem CO_2 (*NEE*) and latent (*LE*) and sensible (*H*) heat exchange were measured using the eddy covariance method (Baldocchi et al., 1988; Baldocchi,

2003) using the same instrumentation as, and following the procedures of, the EUROFLUX project (Aubinet et al., 2000). Briefly, the three wind components and the speed of sound were measured by a three-dimensional sonic anemometer (R2A, Gill Instruments, Lymington, U.K.). CO_2 and H_2O mole fractions were measured by a closed-path infrared gas analyser (Li-6262, Li-Cor, Lincoln, U.S.A.). Air was pumped from the intake, 0.1 m apart from the centre of the sensor volume of the sonic at 3 m height above ground, through a 4 m Teflon tube of 0.004 m inner diameter to the infrared gas analyser at a flow rate 9 l min-1. The infrared gas analyser was operated in the absolute mode, flushing the reference cell with N_2 from a gas cylinder at 100 ml min^{-1}. Raw voltage signals for the CO_2 and H_2O mole fractions were output at 5 Hz to the analogue input of the sonic, where they were synchronised with the sonic signals, which were measured at 20.83 Hz. All raw data were saved to the hard disc of a PC for post-processing using the *Edisol* software (University of Edinburgh). Half-hourly mean fluxes were calculated using the post-processing software *Edire* (University of Edinburgh); the time delay of the CO_2 and H_2O signals was calculated by optimising the correlation coefficient between the respective scalar and the vertical wind velocity (McMillen, 1988). A three-axis co-ordinate rotation was performed aligning the co-ordinate system's vector basis with the mean wind streamlines (Kaimal and Finnigan, 1994), the cross-wind contamination was accounted for according to Schotanus et al. (1983). Raw data were detrended using a running mean with a time constant of 400 s. Finally, frequency response corrections were applied to raw fluxes accounting for low-pass (sensor separation, dynamic frequency sensor response, scalar and vector path averaging, frequency response mismatch, and the attenuation of concentration fluctuations down the sampling tube) and high-pass filtering following Moore (1986) and Aubinet et al. (2000). Net ecosystem exchange (NEE) was calculated as the sum of the corrected vertical covariance term and the storage flux, the latter being estimated from the time rate of change of the scalar concentrations at the reference height, which in a previous comparison with a profiling system was found to be sufficiently accurate. Negative flux densities represent transport towards the surface, positive values the reverse. Half-hourly data were screened for validity by removal of time periods with (i) CO_2 and H_2O signals outside the specified range, (ii) the signal standard deviation to mean ratio exceeding specified limits, and (iii) the third rotation angle exceeding $\pm$ 10° (McMillen, 1988). In contrast to what is often observed with measurements of nighttime *NEE* by means of the eddy covariance technique (Goulden et al., 1996; Jarvis et al., 1997), no decrease of nighttime *NEE* with decreasing atmospheric mixing could be determined at our site despite very little turbulent mixing ($u_* < 0.1$ m s^{-1} during approximately 50% of nighttime), as shown in Figure 1. It rather seems that the intermittent nature of turbulence during these stable and calm conditions primarily acts to greatly increase the sampling error and the run-to-run variability of *NEE*. While this results in considerable scatter in the night time *NEE*, it should not cause a systematic
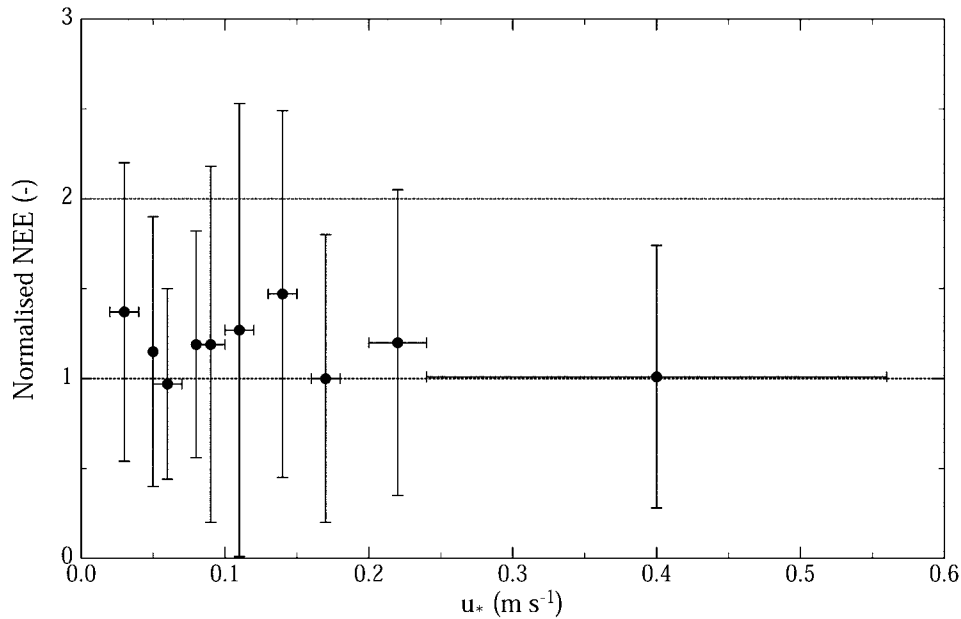
Figure 1. Nighttime *NEE* (normalised by a temperature function; cf. Aubinet et al., 2000) *versus* friction velocity (u_*). Data have been sorted by friction velocity into 10 classes, each with equal number of observations (38). Error bars represent one standard deviation.

underestimation of *NEE* and thus no corrections were applied to nighttime *NEE* data owing to insufficient turbulent mixing (Jarvis et al., 1997).

Additional micrometeorological data were measured as described in Tappeiner et al. (1999). Incoming total and diffuse shortwave radiation were measured using two star pyranometers, net radiation by the means of net radiometers (Schenk, Vienna, Austria). Soil temperatures (0, 0.05, 0.1, 0.2, and 0.5 m) and air temperatures within and above the canopy were measured using thermocouples (copper/constantan, 8×10^{-5} m diameter). Within and above-canopy CO_2 and H_2O concentrations were measured using an infrared gas analyser (CIRAS-Sc, PP-Systems, Hitchin Herts, U.K.) at three heights using a switching manifold. The heights of the within and above canopy scalar concentration measurements were adjusted with canopy development. Soil heat flux was estimated by a combination of the temperature integral method for the upper 0.2 m of the soil and the temperature gradient method for the lower layers of the soil (Gilman, 1977). A recent comparison with soil heat flux plates at this site revealed that this method overestimated soil heat flux measured by heat flux plates (after accounting for heat storage above the heat flux plates) by up to 60%. Based on this comparison a linear correction ($r^2 = 0.80$) was applied to the soil heat flux measured by means of the combination method. The ability of the eddy covariance method to close the energy balance was assessed by plotting the sum of the turbulent energy fluxes ($LE + H$) as a function of available energy ($R_N - G$). The slope and y-intercept (W m^{-2}) of

a linear regression through these data was 1.16 and -21.3 ($r^2 = 0.80$), and 1.05 and -7.9 ($r^2 = 0.86$) before and after applying the above-mentioned correction to the soil heat flux, respectively.

Bulk soil respiration was measured continuously using a steady-state system described in Cernusca and Decker (1989) and an infrared gas analyser (CIRAS-Sc, PP-Systems, Hitchin Herts, U.K.). Soil respiration rates were related to soil temperature measured inside the chamber at 0.05 m depth using an Arrhenius relationship,

$$R_s = R_{s@T\mathrm{ref}} \exp \left[\frac{\Delta H_a}{R T_{\mathrm{ref}}} \left(1 - \frac{T_{\mathrm{ref}}}{T_s} \right) \right], \tag{1}$$

where $R_{s@T\mathrm{ref}}$ is the soil respiration rate (μmol m^{-2} s^{-1}) at the reference temperature (T_{ref}, 293.16 K), T_s the absolute soil temperature (K), R the universal gas constant (8.314 J mol^{-1} K^{-1}) and ΔH_a an activation energy (J mol^{-1}). $R_{s@T\mathrm{ref}}$ and ΔH_a were determined to be 3.19 μmol m^{-2} s^{-1} and 81031 J mol^{-1}, respectively ($r^2 = 0.96$). Residuals were independent of soil moisture (at 0.05 m depth), allowing to neglect any such effects on soil respiration.

2.3. THE SVAT MODEL

The SVAT model employed is a one-dimensional, multi-layer representation of the soil-vegetation-atmosphere continuum and calculates the fluxes of CO_2 and energy between the soil-vegetation system and a given reference height above the canopy. The model has been developed with special emphasis on multi-species mountain grassland ecosystems and is capable of accounting for the separate flux contributions by multiple species and components (Wohlfahrt et al., 2001). It consists of coupled micrometeorological and biophysical/physiological modules: the micrometeorological modules compute radiative transfer (Goudriaan, 1977), the interception of precipitation (Watanabe and Mizutani, 1996), the transfer of momentum (Massman, 1997) and the turbulent dispersion of CO_2, H_2O and sensible heat within and above the canopy. The biophysical/physiological modules solve for the phytoelement energy balance and calculate net photosynthesis, respiration, and stomatal conductance, whenever applicable. Soil heat and water fluxes are simulated with a numerical 10-layer model following Campbell (1985). Since the biophysical/physiological modules depend on the environmental driving forces calculated in the micrometeorological modules, but in turn modify these by the emission of longwave radiation and the exchange of CO_2, H_2O and sensible heat, feedback exists between these two main model compartments.

The SVAT model is similar in structure and function as compared to other contemporary multi-layer SVAT models (Gu et al., 1999; Lai et al., 2000a,b; Baldocchi and Wilson, 2001; Nikolov and Zeller, 2003; Ogee et al., 2003). For a detailed description of the various model components we refer to our previous work (Wohlfahrt et al., 1998, 2000, 2001; Wohlfahrt and Cernusca, 2002), a short summary is

given in Appendix A. In the following we will only treat the theory related to the modelling of turbulent scalar dispersion within and above the plant canopy.

The conservation budget for a passive scalar provides the foundation for computing scalar fluxes and their local ambient concentrations. Assuming steady-state conditions and that the canopy is horizontally homogenous, the change of the vertical flux with height $(\delta F/\delta z)$ equals the (concentration-dependent) source/sink strength $S(C, z)$, i.e.,

$$\frac{\delta F}{\delta z} = S(C, z) = -a(z)\frac{C_a(z) - C_i}{r_b(z) + r_s(z)}. \tag{2}$$

The source/sink strength, in turn, is parameterised using a resistance-analog relationship, where $a(z)$ is the plant area density (PAD, m^2 plant area per m^{-3} canopy volume), $C_a(z) - C_i$ the difference of scalar concentration between the air outside the boundary layer of phytoelements and the air within the stomatal cavity, r_b is the phytoelement boundary layer resistance to molecular diffusion, and r_s is the stomatal resistance ($m\ s^{-1}$). Following Raupach (1989b), scalar concentrations $(C_{a,i})$ may be linked to the source/sink strength (S_j) via a dispersion matrix $(D_{ij}, m\ s^{-1})$,

$$C_{a,i} - C_{a,\text{ref}} = \sum_{j=1}^{n} S_j \Delta z_j D_{ij}, \tag{3}$$

where $C_{a,i} - C_{a,\text{ref}}$ is the concentration difference between an arbitrary level i and the reference height caused by a source/sink S_j in layer j with depth Δz_j (m). For simplicity, in Equation (3) any flux contribution by the soil is lumped to the lowermost canopy layer (Raupach, 1989b).

2.4. LAGRANGIAN DISPERSION MODELS

In the Lagrangian framework a concentration field is related to the statistics of an ensemble of dispersing marked fluid particles. Considering a horizontally homogenous canopy under steady-state conditions with dispersal only in the vertical and provided that turbulent diffusion by far exceeds molecular diffusion, the ensemble-averaged scalar concentration $C(z, t)$ at a given vertical position z and at time t is given by:

$$C(z, t) = \int S(z_0, t_0) P(z, t \mid z_0, t_0)\, dt_0\, dz_0, \tag{4}$$

where $S(z_0, t_0)$ is a source/sink strength of the scalar from a unit volume of phytoelements, $P(z, t \mid z_0, t_0)$ is the transition probability density function that the defines the probability of an air parcel being released at time t_0 from a position z_0 being observed at time t and position z.

2.4.1. *The Random Walk (RW) Model of Baldocchi (1992)*

In the Markov sequence model of Baldocchi (1992) $P(z, t \mid z_0, t_0)$ is evaluated numerically by calculating the trajectories of an ensemble of fluid particles and determining what proportion of fluid particles reside at a given height after travelling for a given time span. The vertical position of a fluid parcel at time t depends on its position at $t - \Delta t$ and on its vertical elocity and is given, in discrete form, by

$$z_{i+1} = z_i + w_i \Delta t, \tag{5}$$

where Δt is the time step increment and w_i the vertical parcel velocity calculated by Thomson's (1987) algorithm for a turbulent flow field, viz.

$$w_{i+1} = w_i + \left[-\frac{w_i}{T_L} + \frac{1}{2} \left(1 + \frac{w_i^2}{\sigma_w^2} \right) \frac{\delta \sigma_w^2}{\delta z} \right] \Delta t + \left(\frac{2\sigma_w^2}{T_L} \Delta t \right)^{1/2} d\Omega, \tag{6}$$

where σ_w is the vertical velocity standard deviation, T_L the Lagrangian time scale, and $d\Omega$ a discrete random increment with zero mean and unit variance. The elements of D_{ij} may be calculated from Equation (3) by following the trajectory of an ensemble of fluid particles, whose source strength is prescribed and uniform with height.

Model domain size, number of released fluid particles, their maximum travel time and the duration between successive time steps were determined in a series of sensitivity tests; the canopy was divided into 20 layers, each initially containing 2500 fluid parcels. The vertical domain over which the particles travelled extended up to 6 m (i.e., two times reference height), or between 9–60 times canopy height, which increased from 0.1 to 0.7 m between DOYs 172 and 225 (Table I). It was assumed that parcels crossing the upper model domain never re-entered. Fluid parcels intercepting the soil surface were perfectly reflected upwards. The maximum travel time was set to 5000 s, the Markov sequence time step equalled 5% of the Lagrangian time scale at canopy height (Baldocchi, 1992).

2.4.2. *The Localised Near-Field (LNF) Theory of Raupach (1989a, b)*

Raupach (1989a, b) decomposed the transition probability density function and the resulting concentrations in Equation (4) into a near-field part, where transport is dominated by persistence, and a far-field part, where transport is essentially diffusive, i.e., $C_a(z) = C_n(z) + C_f(z)$. Assuming that near-field transport can be described as if it occurred in homogenous turbulence with $\sigma_w(z)$ and $T_L(z)$ equal to that at the source height (z_s), the near-field concentration profile, $C_n(z)$, is given by

$$C_n(z) = \int_0^\infty \frac{S(z_s)}{\sigma_w(z_s)} \left\{ k_n \left[\frac{z - z_s}{\sigma_w(z_s) T_L(z_s)} \right] + k_n \left[\frac{z + z_s}{\sigma_w(z_s) T_L(z_s)} \right] \right\} dz_s, \tag{7}$$

TABLE I

Selected canopy properties at the four simulation periods (h = canopy height, PAI = plant area index, ξ = cumulative drag area index, dh^{-1} = normalised zero-plane displacement height, $z_0 h^{-1}$ = normalised momentum roughness length, $z_{\text{ruf}} h^{-1}$ = normalised height of roughness sub-layer, $L_s h^{-1}$ = normalised shear length scale, $T_L(h) u_* h^{-1}$ = normalised Lagrangian time scale at canopy height).

DOY	h (m)	PAI (m² m⁻²)	$\xi(h)$ (m² m⁻²)[a]	dh^{-1} (–)[a]	$z_0 h^{-1}$ (–)[a]	$z_{\text{ruf}} h^{-1} - 1$ (–)[b]	$L_s h^{-1}$ (–)[c]	$T_L(h) u_* h^{-1}$ (–)[b,c]	$T_L(h) u_* h^{-1}$ (–)[a,b]
172	0.10	2.44	0.19	0.38	0.17	2.31	0.89	0.50	0.49
189	0.30	5.47	0.47	0.73	0.07	1.48	0.34	0.19	0.31
207	0.50	7.38	0.62	0.66	0.09	1.64	0.45	0.26	0.36
225	0.70	8.01	0.72	0.61	0.11	1.73	0.51	0.29	0.38

[a] After Massman and Weil (1999).
[b] For neutral stability.
[c] After Raupach et al. (1996).

where k_n is a near-field kernel, whose analytical approximation is derived in Raupach (1989a). Further assuming that far-field transport obeys the gradient-diffusion relationship

$$F(z) = -K_f(z)\frac{\mathrm{d}C_f(z)}{\mathrm{d}z}, \tag{8}$$

the far-field concentration profile, $C_f(z)$, may be found by integrating Equation (8) with height as:

$$C_f(z) = C(z_R) - C_n(z_R) + \int_z^{z_R} \frac{F(z)}{K_f(z)}\mathrm{d}z, \tag{9}$$

where $K_f(z) = \sigma_w^2(z)T_L(z)$ is the so-called far-field diffusivity. The elements of D_{ij} are then defined by the partial concentration profile $C_{a,i}$ obtained by placing a unit source/sink in layer j with zero source/sink in all other layers.

2.4.3. The 'Mixing Matrix' (WT) Model by Warland and Thurtell (2000)

In relating source/sink strength and concentration profiles within a plant canopy, Warland and Thurtell (2000) took a somewhat different approach from that of Raupach (1989a, b) in deriving an analytical solution. Most notably, their model describes dispersion from the near- to far-field continuously and uses turbulence statistics at all heights in both near- and far-field calculations. Their 'mixing matrix' M_{ij} (s m^{-2}) is given as:

$$M_{ij} =$$

$$
\begin{cases}
\dfrac{-\left[1-\exp\left(\frac{-(z_i-z_j)^2}{2\Delta z_j^2}\right)\right]}{2\sigma_{wi}L_{Li}\left[1-\exp\left(-\sqrt{\frac{\pi}{2}}\frac{(z_i-z_j)}{(L_{Li}+L_{Lj})/2}\right)\right]} - \dfrac{\left[1-\exp\left(\frac{-(z_i+z_j)^2}{2\Delta z_j^2}\right)\right]}{2\sigma_{wi}L_{Li}\left[1-\exp\left(-\sqrt{\frac{\pi}{2}}\frac{(z_i+z_j)}{(L_{Li}+L_{Lj})/2}\right)\right]} & \text{for } z_i > z_j \\[3em]
\dfrac{-\left[1-\exp\left(\frac{-(z_i+z_j)^2}{2\Delta z_j^2}\right)\right]}{2\sigma_{wi}L_{Li}\left[1-\exp\left(-\sqrt{\frac{\pi}{2}}\frac{(z_i+z_j)}{(L_{Li}+L_{Lj})/2}\right)\right]} & \text{for } z_i = z_j\,, \\[3em]
\dfrac{\left[1-\exp\left(\frac{-(z_i-z_j)^2}{2\Delta z_j^2}\right)\right]}{2\sigma_{wi}L_{Li}\left[1-\exp\left(-\sqrt{\frac{\pi}{2}}\frac{(z_j-z_i)}{(L_{Li}+L_{Lj})/2}\right)\right]} - \dfrac{\left[1-\exp\left(\frac{-(z_i+z_j)^2}{2\Delta z_j^2}\right)\right]}{2\sigma_{wi}L_{Li}\left[1-\exp\left(-\sqrt{\frac{\pi}{2}}\frac{(z_i+z_j)}{(L_{Li}+L_{Lj})/2}\right)\right]} & \text{for } z_i < z_j
\end{cases}
$$

$$\tag{10}$$

where $L_L = \sigma_w T_L$ is the Lagrangian length scale. In contrast to D_{ij}, which is defined as the concentration difference between level i and the reference level brought about by a unit source in layer j, M_{ij} represents the concentration gradient

across layer i brought about by a unit source in layer j. Using this definition the concentration profile is calculated as:

$$C_{a,i+1} = C_{a,i} + \frac{(z_{i+1} - z_i)}{2} \sum_{j=1}^{n} (M_{i,j} + M_{i+1,j}) S_j. \tag{11}$$

2.4.4. *Turbulence Statistics*

In order to calculate the elements of D_{ij} and M_{ij}, information about the vertical variation of σ_w and T_L is required. Since measurements of σ_w were made only at the reference height, the second-order closure model of Massman and Weil (1999) was used to predict the within- and above-canopy profile of σ_w. The results are shown in Figure 2 for four selected dates distributed evenly across the study period. The corresponding vertical plant area density profiles, derived from linear interpolation between measurement dates, are shown in Figure 3. These four selected dates will be used throughout the remainder of this paper in order to exemplify canopy development during the study period. σ_w is being increasingly more attenuated as the canopy grows (Figure 2), except for DOY 189, when the relatively high PAD in the upper layers causes σ_w to be more strongly attenuated in this region as compared to DOYs 207 and 225. A major difference to many other studies, where σ_w is observed to decrease more or less exponentially with canopy depth (Leuning et al., 2000), is the shape of the σ_w profile, which shows little attenuation in the upper canopy, followed by a linear decrease below. This is due to two central influence variables in the second-order closure model of Massman and Weil (1999), i.e., the vertical PAD profile and the parameterisation of the effective phytoelement drag area coefficient. The vertical PAD profile (Figure 3) resembles a pyramid, the canopy becoming progressively thicker towards the ground, which is typical for mountain grasslands (Tappeiner and Cernusca, 1998). This particular shape, together with the effective phytoelement drag area coefficient increasing with increasing PAD (Wohlfahrt and Cernusca, 2002), result in the observed shape of σ_w. Note also that σ_w was assumed to reach the inertial sub-layer value of $1.25u_*$ already at $z = h$ (Figure 2), where h is the canopy height, since this is implicit in the Massman and Weil (1999) model for T_L, although Raupach et al. (1996) suggest a value of around $1.1u_*$. A sensitivity analysis where σ_w was assumed to increase asymptotically from $1.1u_*$ at $z = h$ to the inertial sub-layer value $1.25u_*$ (following Leuning et al., 2000) showed that this simpler approach underestimated the elements of the dispersion matrix by approximately 5% (data not shown).

Due to the fact that T_L, in contrast to σ_w, cannot be measured directly, the vertical variation of T_L remains somewhat speculative, which is reflected in the fact that three, partially contrasting, parameterisations for the vertical variation of T_L may be found in literature: Raupach (1988) suggested T_L may be approximated as constant within the roughness sub-layer and to increase as $k\,(z - d)/(1.25^2 u_*)$ above, where k is the von Karman constant and d is the zero-plane displacement
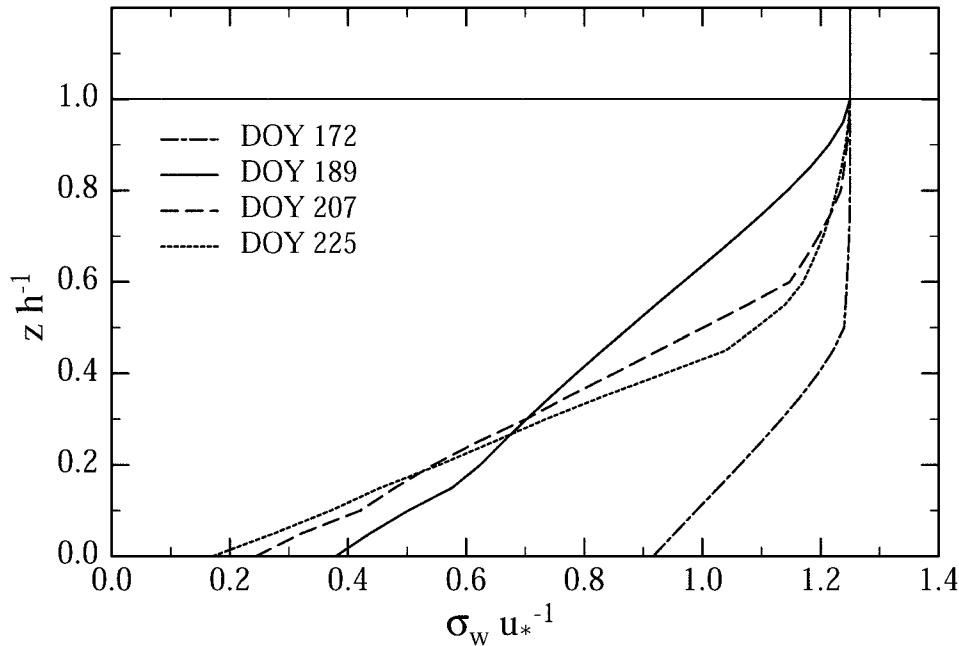
Figure 2. Vertical variation of the normalised vertical velocity standard deviation (σ_w) simulated for neutral conditions with the second-order closure model by Massman and Weil (1999) for the four study dates (referred to by different line types).

height. Leuning et al. (2000) adopted the same shape, but forced T_L to decrease to zero below $z/h = 0.25$. The latter may cause the Markov time step, fixed at 5% of $T_L(h)$, to exceed T_L close to the soil surface during random walk simulations. While in principle it would be possible to determine the maximum allowable time step, this would cause an excessive computational overhead, which seems not justified given that varying the time step between 10-1% of $T_L(h)$ causes less than 4% difference to the dispersion matrix. Massman and Weil (1999) assumed $T_L \propto \sigma_w^{-1}$ within the canopy, which results in T_L increasing towards the ground. These three parameterisation options, separately for each study date, are shown in Figure 4. In the Raupach (1988) and Leuning et al. (2000) parameterisations, $T_L(h)u_*h^{-1}$ was calculated according to Raupach et al. (1996) as $0.71L_s/(1.25h)$, where L_s is a turbulence length scale (Table I) calculated as $u(h)/u'(h)$, where $u(h)$ is the mean wind velocity and $u'(h) = du/dz$, both at $z = h$. As noted already by Massman and Weil (1999), $T_L(h)u_*h^{-1}$ predicted by their model is close to the formulation by Raupach et al. (1996) at cumulative drag area indices ($\xi(h)$) between 0.2–0.3 (e.g., DOY 172), but higher as $\xi(h)$ increases (Figure 4, Table I).

The parameterisation of σ_w and T_L as discussed above is appropriate for neutral atmospheric conditions, but requires modification for unstable and stable conditions. Here we adopt the approach of Leuning (2000), who developed stability corrections for σ_w and T_L based on the stability functions for heat and velocity
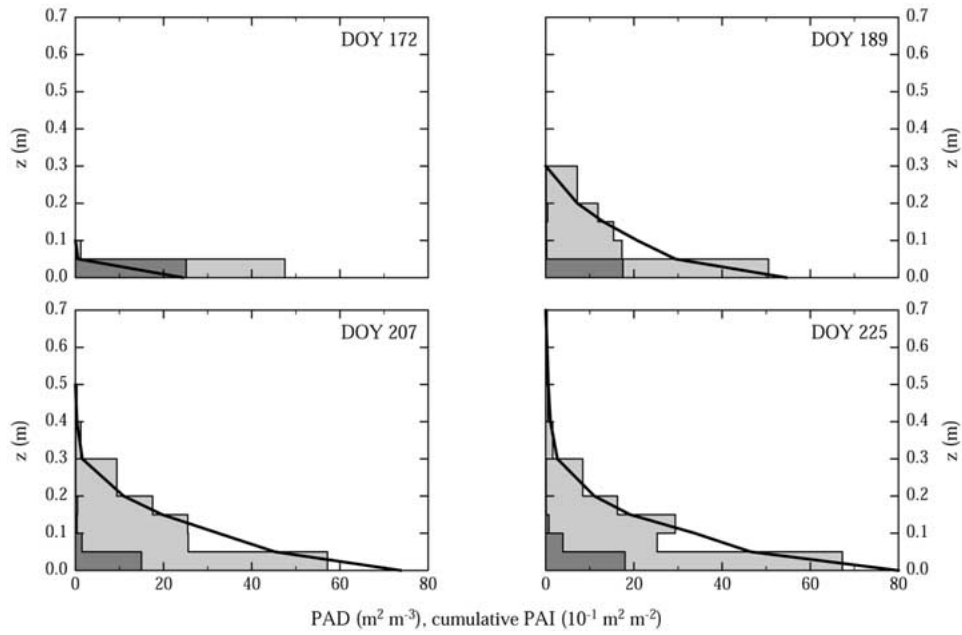
Figure 3. Vertical plant area density distribution (shaded areas) and cumulative plant area index (thick solid line) for the four study dates. Light grey areas refer to photosynthetically active, dark grey areas to photosynthetically inactive plant material.
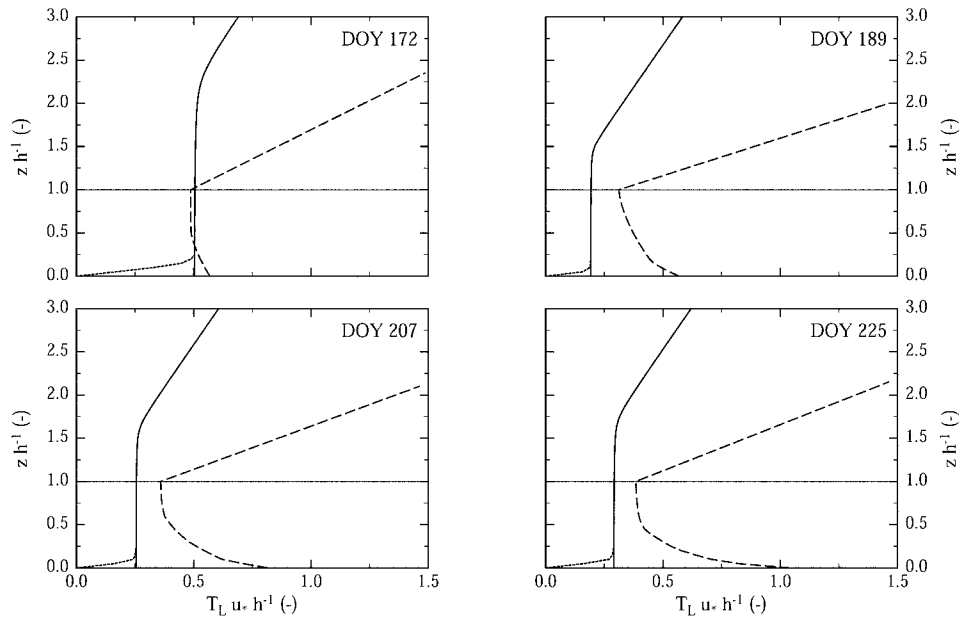
Figure 4. Vertical variation of the normalised Lagrangian time scale (T_L) for the four study dates (neutral conditions). Solid lines refer to the Raupach (1988), dotted lines to the Leuning et al. (2000), and broken lines to the parameterisation after Massman and Weil (1999).
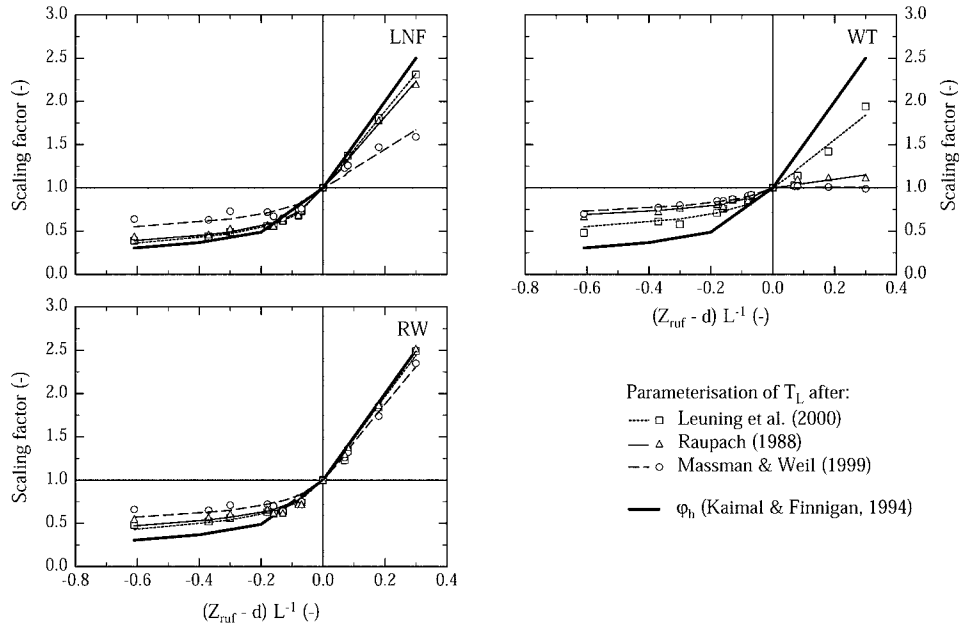
Figure 5. Parameterisation of the stability dependence of the dispersion matrix scaling factor as described in the text. Simulations have been conducted for the LNF, WT and RW model using a friction velocity of 0.5 m s^{-1}. Solid lines and triangles refer to the Raupach (1988), dotted lines and squares to the Leuning et al. (2000), and broken lines and circles to the Massman and Weil (1999) parameterisation of T_L. The stability function for heat (after Kaimal and Finnigan, 1994) is shown for reference (thick solid lines).

variance given in Kaimal and Finnigan (1994). In contrast to Leuning (2000), who defined the stability parameter, ζ, as h/L within the roughness sub-layer and as $(z - d)/L$ above, where L is the Obukhov length, we, as Ogee et al. (2003), use $(z_{\mathrm{ruf}} - d)/L$ both within and above the roughness sub-layer, where z_{ruf} is the height of transition from the roughness sub-layer to the inertial layer (Leuning et al., 2000). We note (i) that there are no theoretical or experimental guidelines as to the form of the stability functions below z_{ruf}, and (ii) that according to Leuning (2000) fluxes exhibit little sensitivity to the choice of length scale, which was confirmed in a series of sensitivity tests with our model (data not shown). The main advantage (from a modeller's point of view) of using a fixed length scale is that this allows stability effects to be included by means of a simple scaling factor (Baldocchi and Harley, 1995; Ogee et al. 2003), as shown in Figure 5. The scaling factors in Figure 5 are the slopes of several linear regressions (with zero intercept) of the elements of the dispersion/mixing matrices calculated for various values of ζ against the respective matrix elements for neutral stability. Lines in Figure 5 represent best fits to these data using:

$$\phi(\zeta) = \begin{cases} (1 + a|\zeta|)^b & \zeta \leq 0 \\ (1 + c\zeta) & \zeta > 0 \end{cases}, \tag{12}$$

TABLE II

Parameterisation of the stability dependence of the scaling coefficient using Equation (12) as explained in the text. Parameter a has been held constant at 16.

Model	T_L parameterisation	b	c	r^2
LNF	Leuning et al. (2000)	−0.42	4.33	1.00
	Raupach (1988)	−0.40	4.05	1.00
	Massman and Weil (1999)	−0.25	2.20	0.96
WT	Leuning et al. (2000)	−0.25	2.74	0.96
	Raupach (1988)	−0.16	0.50	0.97
	Massman and Weil (1999)	−0.13	0.03	0.98
RW	Leuning et al. (2000)	−0.35	4.74	1.00
	Raupach (1988)	−0.32	4.89	0.99
	Massman and Weil (1999)	−0.24	4.29	0.99

where the respective parameters, separately for each of the three models and the three parameterisation options for T_L, are given in Table II. Using Equation (12), effects of stability and friction velocity on turbulent transport may be accounted for by scaling a reference dispersion/mixing matrix, valid for an arbitrary reference friction velocity (u_*^{ref}) and neutral stability, to stability and friction velocity using:

$$D_{ij}(u_*, \zeta) = D_{ij}^{\text{ref}} \phi(\zeta) u_*^{\text{ref}} / u_*. \tag{13}$$

Several interesting features are evident from Figure 5. First, the stability dependences of the three models differ; the stability dependence of the LNF theory and the random walk model are fairly close to the stability function of heat (ϕ_h; Kaimal and Finnigan, 1994). This is not surprising in the case of the LNF theory, where the stability dependence of the far-field part reduces to that of ϕ_h, while no simple relationship exists for the near-field part. Since near-field effects, as critiqued by Warland and Thurtell (2000), play a relatively minor role in the LNF theory, this is merely a manifestation of the model's weight on far-field effects. Conversely, the stability dependence of the WT model deviates considerably from that of ϕ_h, even though both models have the same far-field limit, due to the improved consideration of near-field effects. Surprisingly, the closest correspondence with ϕ_h is observed for the random walk model, despite the fact that it incorporates neither of the simplifications of the two analytical models. Second, the stability dependences of the three parameterisation options for T_L differ too, the stability dependence using the parameterisation after Raupach (1988) and Leuning et al. (2000) being fairly similar and closer to ϕ_h than the one after Massman and Weil (1999), which in the case of the WT model shows hardly any change with ζ on the stable side (Figure 5).
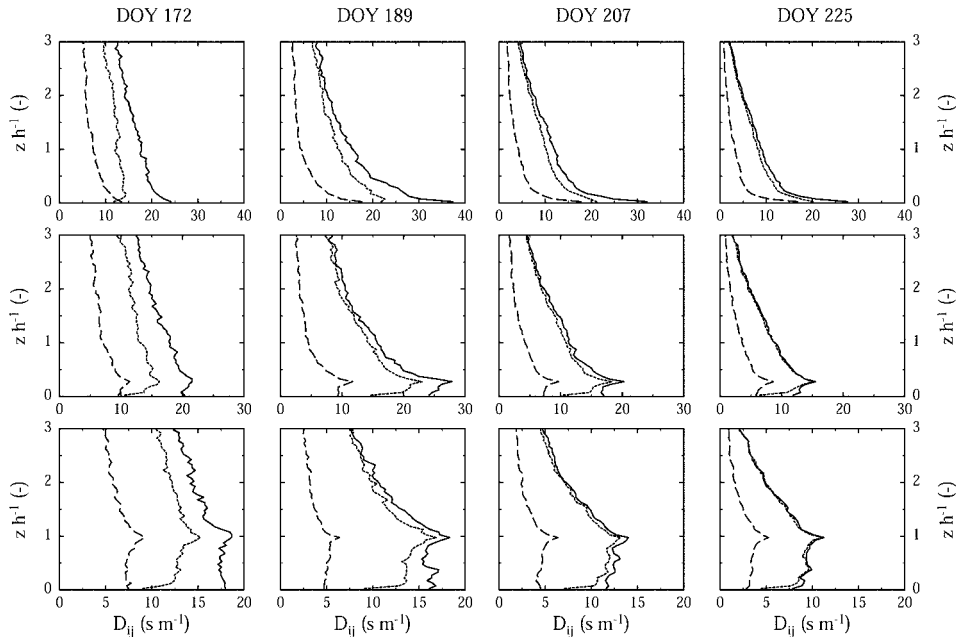
Figure 6a. Vertical variation of the elements of the dispersion matrix (D_{ij}) calculated with the RW model for a friction velocity of 0.5 m s^{-1} and neutral stability. Source heights are $z = 0$, $z = 0.25h$ and $z = h$ in the upper, middle and lower panel, respectively. Line symbols are the same as in Figure 4. Note the different scales on the x-axis.

3. Results

In a first step, it is instructive to compare the three Lagrangian models and parameterisation options for T_L without the complexity of spatially and temporally varying source/sink distributions, i.e., by comparing the dispersion matrices. Figures 6a–c show these for the RW, LNF and WT model and source heights $z = 0$, $z = 0.25h$ and $z = h$ in the upper, middle and lower panel, respectively. Note that for the purpose of comparing the three models, the WT mixing matrices in Figure 6c have been manipulated to be compatible with Equation (3) and thus directly comparable to the LNF and RW dispersion matrices.

Profiles predicted by the two analytical models (LNF and WT) are much smoother than those of the RW model, reflecting numerical noise associated with the simulation of particle trajectories (Raupach, 1989a). Except for this, the profiles have generally similar shapes: the values of the dispersion matrices are generally largest at the source height, resulting in more or less prominent discontinuities in the profile (Figures 6a–c). This implies that the largest contribution by each source/sink is to the concentration at that respective height and accordingly less to the other canopy layers. An exception to this general pattern are the WT dispersion matrices for source heights $z = h$ at DOYs 172, 207 and 225 (Figure 6c), where
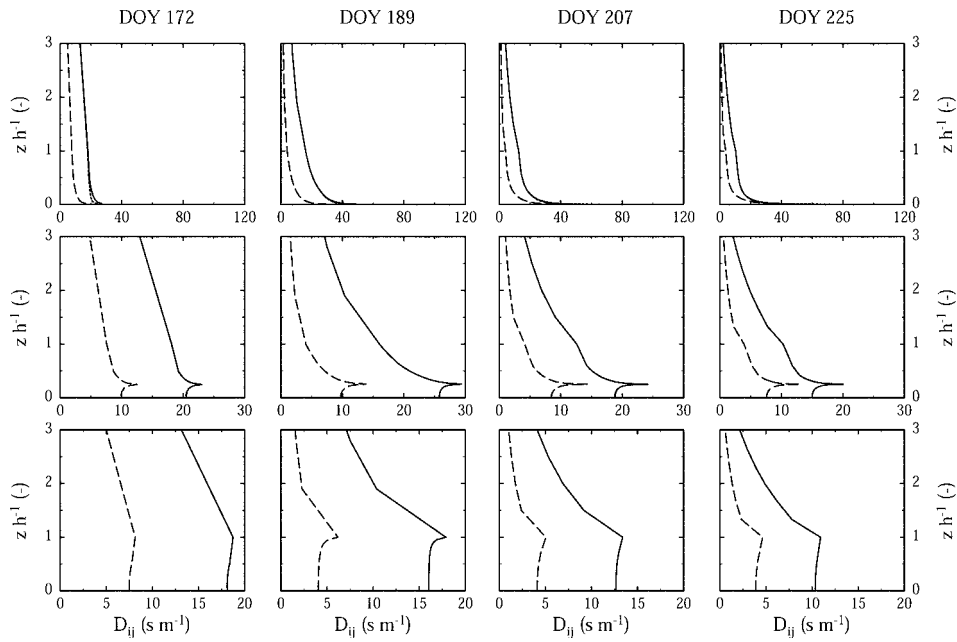
Figure 6b. Same as Figure 6a, but for the LNF model.
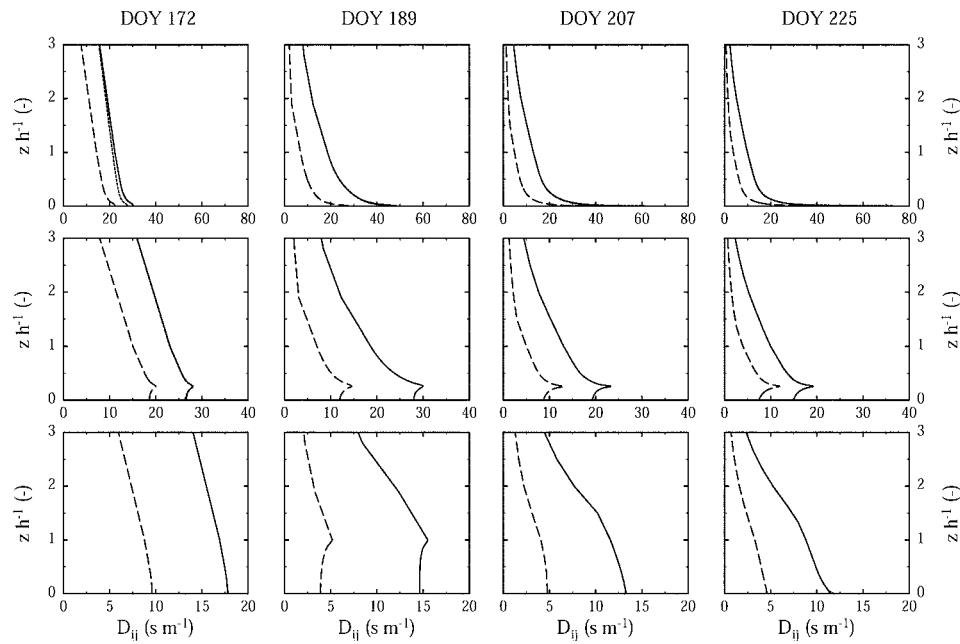
Figure 6c. Same as Figure 6a, but for the WT model.

the image source (second term on right-hand side of Equation (10)), offsets this effect. The magnitude of the elements of the dispersion matrices are similar in all three models, except close to the soil surface where the LNF theory predicts values up to 3 times as high as the RW model (Figures 6a–c).

The effect the three different parameterisation options for T_L have on the dispersion matrices depends partly on model theory. With the LNF and WT models, differences between the Raupach (1988) and Leuning et al. (2000) parameterisation of T_L occur only for source heights close to the soil surface (Figures 6b and c), where the parameterisations also differ, while the RW model yields different dispersion matrices for any source height (Figure 6a). The latter differences diminish, i.e., simulations with the Raupach (1988) and Leuning et al. (2000) parameterisation of T_L become increasingly similar, as the canopy grows (Figure 6a). Clear differences are observed between the latter two parameterisations of T_L and the one by Massman and Weil (1999), which yields smaller values independent of model theory and canopy development (Figures 6a–c).

In a second step we analyse the performance of the three models and parameterisation options for T_L in simulating scalar concentration profiles, by comparison with concentration measurements at various heights within and above the canopy: Differences between the investigated model/parameterisation combinations in their ability to predict scalar concentrations are fairly small, and clearly smaller than the difference between the respective model predictions and measurements (Table III). If anything, it appears that the Massman and Weil (1999) parameterisation of T_L performs slightly less well compared to the other two parameterisation options, and that the correspondence between model and measurements is somewhat more favourable for the LNF and WT, as compared to the RW model (Table III). Given the similar suitability of the three models and parameterisation options for predicting scalar concentrations, we restrict the following comparison of measured and simulated concentration profiles (Figure 7) to an arbitrary combination of model theory and T_L parameterisation, e.g., the LNF model with Raupach's (1988) parameterisation of T_L.

Air temperatures are predicted correctly above and within the upper part of the canopy, but tend to be overestimated by up to 3 °C during nighttime and underestimated by up to 8 °C during daytime in the lower canopy layers (Figure 7, upper panels). In the latter case, temperatures are too uniform with height as compared to measurements, which suggest an increase towards the surface (DOY 172 and 189) and a local air temperature maximum at around $z/h = 0.4$ for DOYs 207 and 225. The correspondence between measured and simulated water vapour partial pressures is similar as compared to air temperature, being overestimated during nighttime (up to 3 hPa) and underestimated (up to 7 hPa) during daytime, but far fewer data are available for comparison (Figure 7, central panels). CO_2 concentration profiles are generally well predicted, except for close to the soil surface, where measurements exceed modelled concentrations during day- and night time by up

TABLE III

Statistics for comparison between measured and simulated scalar concentrations. Simulations have been conducted using the RW, LNF and WT model and three different options for the parameterisation of T_L. Model performance is evaluated by the slope and y-intercept of a linear regression, the root mean squared error (RMSE) and the Pearson's correlation coefficient (r). Numbers are dimensionless except for the y-intercept and the RMSE, which have units of °C (T_{air}), hPa (E_{air}) and μmol mol^{-1} (C_{air}). The number of half-hourly samples is 720, 208 and 304 for T_{air}, E_{air} and C_{air}, respectively.

Model	Scalar	Leuning et al. (2000)				Raupach (1988)				Massman and Weil (1999)			
		Slope	y-Intercept	RMSE	r	Slope	y-Intercept	RMSE	r	Slope	y-Intercept	RMSE	r
RW	T_{air}	0.87	2.10	2.10	0.98	0.87	2.26	1.99	0.99	0.87	2.05	2.12	0.98
	E_{air}	0.87	1.29	2.09	0.96	0.90	0.92	1.79	0.97	0.86	1.37	2.00	0.97
	C_{air}	0.57	163.10	112.02	0.88	0.60	152.04	107.91	0.89	0.57	166.01	112.84	0.88
LNF	T_{air}	0.86	2.46	2.09	0.99	0.86	2.53	2.10	0.98	0.86	2.42	2.15	0.98
	E_{air}	0.86	1.54	1.76	0.97	0.86	1.56	1.76	0.97	0.85	1.62	1.92	0.97
	C_{air}	0.65	133.95	98.95	0.90	0.65	134.97	99.10	0.90	0.60	152.88	106.76	0.88
WT	T_{air}	0.86	2.47	2.09	0.99	0.87	2.33	2.05	0.99	0.87	2.20	2.11	0.98
	E_{air}	0.87	1.50	1.77	0.97	0.87	1.40	1.78	0.97	0.85	1.45	1.96	0.97
	C_{air}	0.63	142.15	102.04	0.90	0.61	147.60	104.60	0.89	0.58	161.60	110.36	0.88
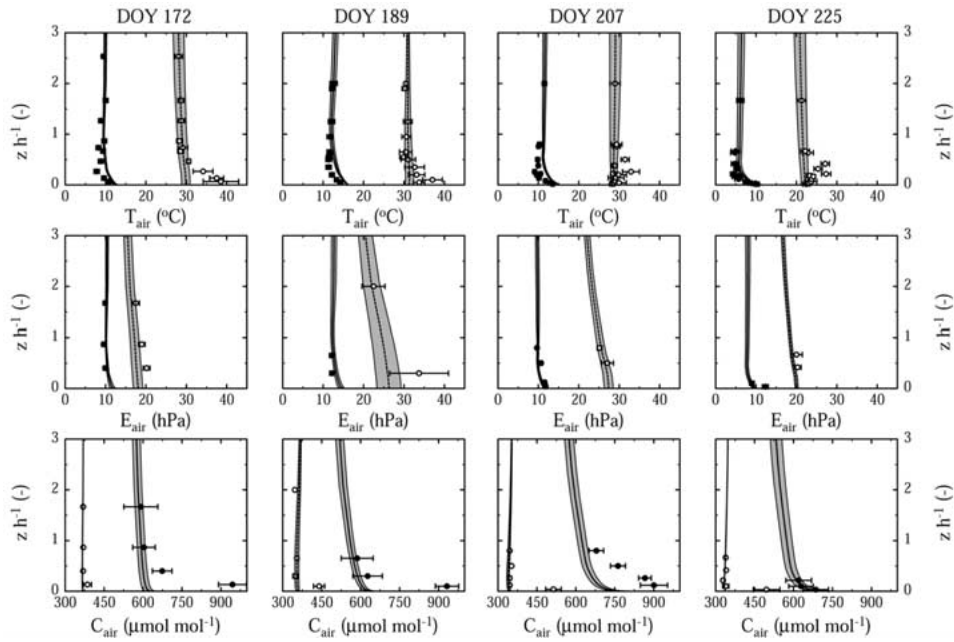
Figure 7. Comparison between measured and simulated profiles of CO_2 concentration (C_{air}), water vapour pressure (E_{air}) and air temperature (T_{air}). Simulations have been conducted with the LNF theory and the Raupach (1988) parameterisation of T_L and represent bin-averages for five days centred around the study dates. Closed symbols and solid lines refer to nighttime, open symbols and dotted lines to daytime conditions. Error bars represent one standard deviation of measurements, shaded areas one standard deviation of model results.

to 150 and 300 μmol mol^{-1}, respectively (Figure 7, lower panels). For night time conditions this underestimation tends to diminish with canopy development.

Next we compare the output of simulations with the investigated model/parameterisation combinations with measured net radiation, sensible, latent and soil heat fluxes, as well as net ecosystem CO_2 exchange. Similar to the previous model validation, differences with regard to the correspondence to measured ecosystem fluxes are subtle, none of the model/parameterisation combinations being quantitatively or qualitatively clearly superior, and again these differences are smaller than the differences between the respective model predictions and measurements (Table IV). Similar to the validation of the concentration profiles, the Massman and Weil (1999) parameterisation appears to result in a larger deviation between model and measurements. In the absence of a clearly superior model/parameterisation combination, we thus again restrict the detailed assessment of model performance to an arbitrary combination of model theory and T_L parameterisation, e.g., the LNF model with Raupach's (1988) parameterisation of T_L (Figure 8).

Qualitative correspondence between measured and modelled *NEE* is fairly good at all dates, except for DOY 172, although a systematic underestimation (approxi-

TABLE IV

Statistics for comparison between measured and simulated ecosystem fluxes. Simulations have been conducted using the RW, LNF and WT model and three different options for the parameterisation of T_L, as well as the half-order closure (HOC) model. Model performance is evaluated by the slope and y-intercept of a linear regression, the root mean squared error (RMSE) and the Pearson's correlation coefficient (r). Numbers are dimensionless except for the y-intercept and the RMSE, which have units of W m^{-2} (LE, H, R_N, G) and μmol m^{-2} s^{-1} (NEE). The number of half-hourly samples is 805, 898, 912, 960 and 950 for NEE, LE, H, R_N and G, respectively.

Model	Scalar	Leuning et al. (2000)				Raupach (1988)				Massman and Weil (1999)			
		Slope	y-Intercept	RMSE	r	Slope	y-Intercept	RMSE	r	Slope	y-Intercept	RMSE	r
RW	NEE	0.98	−4.77	7.07	0.90	0.97	−4.52	6.78	0.91	0.98	−4.76	6.85	0.91
	LE	0.89	23.72	44.73	0.93	0.89	21.34	44.96	0.93	0.90	27.23	51.46	0.92
	H	0.75	−1.74	22.93	0.89	0.69	0.76	23.57	0.89	0.87	−5.52	24.81	0.88
	R_N	1.00	2.64	11.54	1.00	0.99	2.07	12.35	1.00	1.01	2.89	11.80	1.00
	G	0.70	0.03	26.37	0.81	0.74	0.81	26.27	0.82	0.67	−0.12	26.94	0.80
LNF	NEE	0.98	−4.63	6.74	0.91	0.98	−4.62	6.75	0.91	0.98	−4.79	6.87	0.91
	LE	0.89	21.36	47.45	0.92	0.90	19.98	42.94	0.94	0.91	24.98	50.05	0.92
	H	0.72	2.67	23.90	0.87	0.72	2.68	21.83	0.90	0.88	−3.09	24.24	0.88
	R_N	1.00	3.44	11.16	1.00	1.00	3.19	10.61	1.00	1.02	3.63	11.73	1.00
	G	0.70	0.41	26.82	0.81	0.70	0.51	26.70	0.81	0.65	−0.05	27.60	0.79
WT	NEE	0.98	−4.60	6.72	0.91	0.97	−4.58	6.72	0.91	0.98	−4.80	6.87	0.91
	LE	0.90	19.33	41.53	0.94	0.90	19.50	41.48	0.94	0.91	25.86	50.26	0.92
	H	0.72	2.49	21.69	0.90	0.71	2.09	21.67	0.90	0.87	−4.20	24.73	0.88
	R_N	1.00	2.81	10.66	1.00	1.00	2.08	11.33	1.00	1.02	3.30	11.54	1.00
	G	0.70	0.51	26.59	0.81	0.71	0.51	26.46	0.81	0.66	−0.18	27.43	0.79
HOC	NEE	0.99	−4.68	6.83	0.91								
	LE	0.86	44.43	94.48	0.76								
	H	1.28	−25.37	79.96	0.64								
	R_N	1.03	2.06	13.52	1.00								
	G	0.61	−0.59	29.15	0.76								
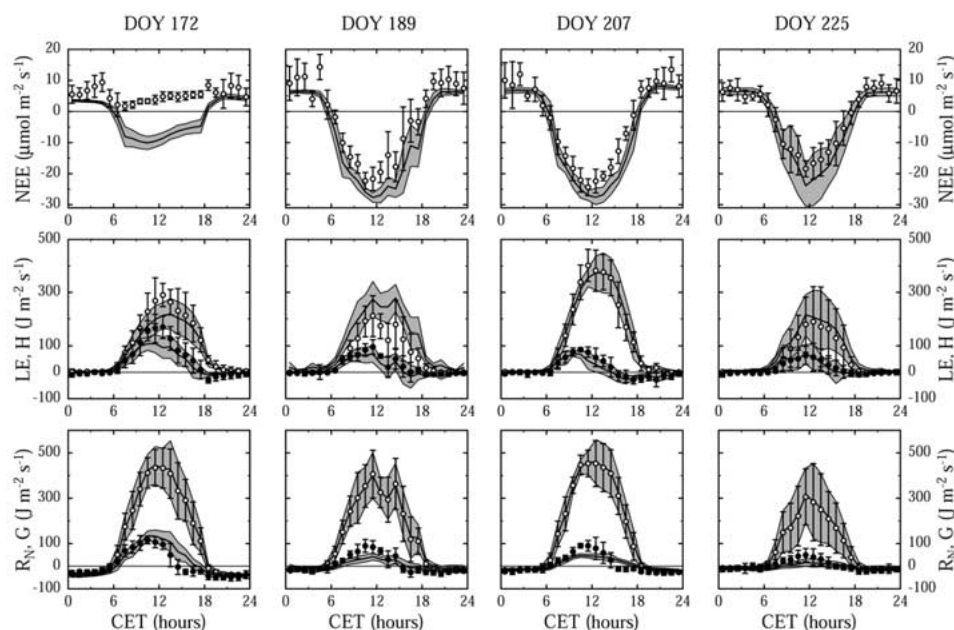
Figure 8. Comparison between measured and simulated net ecosystem CO_2 exchange (NEE), latent (*LE*), sensible (*H*), and soil heat (*G*) fluxes and net radiation (R_N). Simulations have been conducted with the LNF model and the Raupach (1988) parameterisation of T_L and represent hourly bin-averages for five days centred around the study dates. Closed symbols and solid lines refer to sensible heat and soil heat fluxes, open symbols and dotted lines to latent heat fluxes and net radiation in the middle and lower panels, respectively. Error bars represent one standard deviation of measurements, shaded areas one standard deviation of model results.

mately -4.6 μmol m^{-2} s^{-1}), which decreases with canopy development, is evident (Figure 8, Table IV). Immediately after the first cut (DOY 172), considerable divergence between measured and modelled NEE is observed – measured *NEE* remains positive all day long, while modelled *NEE* shows a clear net CO_2 uptake (up to -10 μmol m^{-2} s^{-1}) during daytime. Latent heat fluxes are underestimated on DOY 172, overestimated on DOY 189, and agree reasonably with measurements on DOYs 207 and 225 (Figure 8). Sensible heat fluxes are generally underestimated, in particular on DOY 172 and 207 (Figure 8, Table IV). Correspondence between measured and predicted net radiation is almost perfect during all four simulation periods, while soil heat flux is increasingly being underestimated with canopy development (Figure 8, Table IV).

Finally, it is instructive to assess how well ecosystem fluxes are predicted by adopting a half-order closure approach, i.e., by assuming that scalar concentrations are constant with height. As shown in Table IV, net ecosystem CO_2 exchange and net radiation predicted by the half-order closure approach are qualitatively and quantitatively almost identical to the predictions by the Lagrangian models. In the case of latent, sensible and soil heat flux predictions though, Table IV shows that

correspondence with measured data is clearly less favourable for the half-order closure model. This is primarily due to sensible heat being underestimated and latent heat being overestimated during the afternoon (data not shown).

4. Discussion

It is now commonly acknowledged that the effects of persistence caused by the correlated nature of turbulence precludes the use of a so-called eddy diffusivity (K-theory) to model turbulent dispersion within plant canopies (Raupach, 1987; Raupach et al., 1996). The price for physically realistic predictions of within-canopy flow is usually a good deal of extra complexity associated with models suitable for this purpose, i.e., second- and higher-order closure, as well as Lagrangian models. It is thus legitimate to explore how much detail is required to successfully predict the canopy microclimate and fluxes. A major attempt at this was made by Raupach (1989a, b), who proposed the localised near-field (LNF) theory as a simple and computationally efficient alternative to Lagrangian random walk models. Recently, Warland and Thurtell (2000) improved upon this concept, by relaxing some of the assumptions inherent to the LNF theory. These two models, together with the random walk model by Baldocchi (1992), which, as compared to the two analytical models, contains the least amount of approximations, are compared in the present paper. The issue of model theory is combined with a practical one, namely the choice of the Lagrangian time scale, which, since it cannot be measured directly, must either be deduced from its Eulerian counterpart (Katul et al., 1997) or, as it is most often the case, estimated.

4.1. MODEL INTERCOMPARISON

One of the major results of the comparison of the three investigated Lagrangian models is that differences in their ability to predict scalar concentrations and ecosystem fluxes are close to being indistinguishable. Findings along this line have been reported also by Wilson et al. (2003), who compared the ability of the LNF and WT model to predict energy fluxes and air temperatures above and within a potato crop. More or less identical CO_2 and energy fluxes have been observed also by Baldocchi (1992), who compared the random walk algorithms of Thomson (1987) and Legg and Raupach (1982) in a soybean crop. In this study Baldocchi (1992) also found that the Legg and Raupach (1982) algorithm, despite acknowledged limitations, resulted in concentration profiles which were in closer agreement with measurements as compared to the Thomson (1987) algorithm. Warland and Thurtell (2000) found their model, as compared to the LNF theory, to better capture air temperatures close to the (prescribed) heat source in a wind-tunnel experiment, but overall differences between both models were again relatively small. We may thus conclude that the theoretical differences between

the three Lagrangian models, or more generally between different turbulent diffusion models, play a negligible role, as long as the overall shape and approximate magnitude of scalar concentrations are captured, since the sensitivity of ecosystem fluxes to scalar concentrations is apparently fairly low. Similar conclusions, but with regard to the performance of K-theory, have been reached by Dolman and Wallace (1991), Van den Hurk and McNaughton (1995), McNaughton and Van den Hurk (1995) and Wilson et al. (2003). Here we note, that the differences in computational efficiency between K-theory and the WT model, the computationally most efficient of the three investigated models, are likely to be insignificant as to justify the ignorance of the well established limitations of K-theory. The apparent insensitivity, should though not lead us to conclude that the provision of turbulent dispersion in SVAT models is redundant. The half-order closure simulations (Table IV) clearly show that, at least for correctly predicting energy fluxes, turbulent diffusion needs to be accounted for, which has been corroborated by Baldocchi (1992, 1993), Baldocchi and Wilson (2001) and Ogee et al. (2003) amongst others. These studies also confirm that net ecosystem CO_2 exchange may well be predicted with sufficient precision using a half-order closure approach, which is due to the fact that CO_2 concentrations within the canopy are usually close to ambient except for close to the soil surface. In this region of the canopy most of the leaves are shaded, receiving diffuse light only, while a small fraction of sunlit leaves receives both direct and diffuse radiation (Ross, 1981). Shaded leaves are thus usually limited with regard to the availability of photosynthetically active radiation and are unable to exploit the high CO_2 concentrations in a manner comparable to sunlit leaves (Baldocchi, 1993). The consequences of the underestimation of CO_2 concentrations by assuming a constant value thus remain negligible and are partially compensated by the overestimation of photosynthesis in the upper canopy layers, where a draw down of CO_2 below ambient usually takes place.

4.2. THE PARAMETERISATION OF THE LAGRANGIAN TIME SCALE

If we follow Raupach et al. (1996) in assuming that $T_L = L_w \sigma_w^{-1}$, where L_w is the Lagrangian horizontal length scale of vertical velocity (deduced from its Eulerian counterpart), the three profiles of T_L tested in the present paper are all possible, depending on whether σ_w attenuates faster than e.g., the Massman and Weil (1999) parameterisation, and similar to e.g., the Raupach (1988) parameterisation, or more slowly e.g., the Leuning et al. (2000) parameterisation) than L_w with canopy depth. The 'family curves' of Raupach et al. (1996) confirm the existence of these three general shapes, but the estimated length scales must be viewed with caution, given that they are based on single-point turbulence statistics, which have been shown to be smaller than two-point length scales by factors of two and more within the canopy by the same authors. Given the uncertainties associated with the estimation of T_L, as well as the fact that all three parameterisations appear plausible, but that we lack a means of judging their suitability for the present study, it is fortunate

that our simulations indicate that the sensitivity to the choice of the shape of T_L is relatively small, which corresponds with sensitivity test by Raupach (1987, 1989b), Baldocchi (1992) and Lai et al. (2002). While the results obtained in the present study with the Raupach (1988) and Leuning et al. (2000) parameterisations are similar, which is not surprising given they are identical except for $z/h < 0.25$, it appears that the Massman and Weil (1999) model, characterised by T_L increasing towards the ground and up to 60% higher T_L values at $z = h$ (Figure 5), is less suited for the investigated canopies. It should though be mentioned that the Massman and Weil (1999) model of T_L was successfully employed, e.g., by Ogee et al. (2003) in a maritime pine and by Marcolla et al. (2003) in a mixed coniferous forest.

4.3. MODEL VALIDATION

Overall, quantitative and qualitative statistics for the comparison between measured and simulated ecosystem fluxes are similar to what has been reported by other modellers (Baldocchi and Harley, 1995; Williams et al., 1996; Baldocchi and Meyers, 1998; Gu et al., 1999; Lai et al., 2000a, b, 2002a, b; Baldocchi and Wilson, 2001; Baldocchi et al., 2002; Ogee et al., 2003; Wilson et al., 2003), model predictions corresponding to within $\pm 30\%$ and capturing 80% of the variance of field measurements (Baldocchi and Wilson, 2001).

The present simulations capture the diurnal trend of measured *NEE* well (except for DOY 172), as indicated by slopes close to unity, but the negative y-intercepts of around -4.6 μmol m^{-2} s^{-1} indicate a systematic underestimation. While there are many potential reasons for this discrepancy, we believe it is largely due to an underestimation of soil respiration associated with our steady-state soil respiration measurements. Recent measurements with a non-steady-state system suggest significantly higher soil respiration rates, than those used to parameterise Equation (1) (M. Bahn, personal communication, 2003), which is in contrast to the notion that closed, non-steady-state systems tend to underestimate soil respiration (Rayment, 2000). While the chamber vent should have prevented any overpressure from developing inside the chamber, it might be that the underestimation with the steady-state system is due to a reduced diffusion gradient caused by insufficient mixing of chamber air (Davidson et al., 2002), which is not ventilated, except for the through-flow. Until this methodological issue is resolved and the absolute magnitude of soil respiration at this site determined with confidence, we consider the present parameterisation of soil respiration as a working hypothesis, which likely requires adjustment towards higher values.

There are two reasons for the model to predict daytime CO_2 uptake on DOY 172: first, while greatly reduced due to cutting, there is still enough assimilating plant material available (Figure 3), and second, due to reduced self-shading within the canopy, light availability is greatly enhanced as compared to before cutting, which in combination results in the predicted daytime CO_2 uptake. The reduction

of measured CO_2 losses during the cool morning hours indeed suggests some assimilatory activity, which is though offset by an increase in respiratory losses as temperatures rise. An underestimation of soil temperature is not the cause for the observed underestimation of respiration, since measured and predicted soil temperatures compare fairly well (linear regression: $T_{predicted} = 0.95 \cdot T_{measured} + 1.38$, $r^2 = 0.95$), which in turn suggests that above- and/or below-ground respiratory capacities are underestimated. Enhanced respiration rates might be caused by several processes, e.g., repair processes in the injured plant material, the production of new biomass (Larcher, 2001), rapid decomposition of fresh litter, and enhanced diffusion of CO_2 out of the soil as a result of the increased soil-atmosphere CO_2 gradient created by the removal of most of the above-ground plant material (Figure 7).

Excellent correspondence with measured data is achieved for net radiation, which provides an integrated test for the model of radiative transfer and the energy balance and should be computed accurately if we hope to partition energy fluxes correctly. Note that in contrast to Baldocchi and Harley (1995), no clumping factor needed to be invoked in order to match measured net radiation, providing further '*a posteriori*' justification for the assumption of a random phytoelement dispersion (Wohlfahrt et al., 2000).

Latent heat fluxes are generally underestimated by between 9–11%, but overestimation occurs as well, e.g., around DOYs 189 and 225 (Figure 8, Table IV). The fact that latent heat fluxes are underestimated after cutting, presents further evidence that net photosynthesis is predicted correctly around DOY 172, since stomatal conductance is linearly related to net photosynthesis in the stomatal model of Ball et al. (1987) (cf. Equation (A2) in Appendix A). Any overestimation of net photosynthesis should thus cause a proportional overestimation of transpiration. The underestimation of latent heat fluxes around DOY 172, thus rather suggests that soil evaporation is somewhat underestimated during times with little canopy cover.

Sensible and soil heat fluxes are usually much more difficult to model accurately than latent heat (at least for well-watered ecosystems) and net radiation, resulting in less correspondence with measured data (Raupach et al., 1997), as in the present study, where they are underestimated by 12–31 and 26–35%, respectively. The failure to correctly predict sensible heat fluxes may be to some extent attributable to the use of phytoelement boundary layer conductance algorithms derived from measurements on flat plates under controlled, steady environmental conditions (Schuepp, 1993). The best one can currently do in order to at least partially account for the unsteady turbulent nature of the canopy environment is to use a beta multiplier (Campbell and Norman, 1998). In addition, phytoelement boundary-layer resistances are typically much smaller than the resistance to diffusion of water vapour through stomatal pores. Sensible heat fluxes are thus fairly sensitive to any errors in the leaf to air temperature gradient (Baldocchi and Harley, 1995), which is

demonstrated impressively by the degradation of sensible heat statistics when the half-order closure model is used (Table IV).

Soil heat fluxes depend on the energy exchange at the soil-to-air interface, possibly with a litter layer sandwiched in between, and the heat and water movement within the underlying soil (Ogee and Brunet, 2002). Solving the soil surface energy balance is more complicated as compared to phytoelements due to significant heat storage (Campbell, 1985), and the fact that the surface conductance depends in a complex fashion on water availability (Mahfouf and Noilhan, 1991). In mountain grasslands, where the soil surface is covered by a dense vegetation cover which largely precludes any non-obstructive measurements, these theoretical problems are reinforced by a lack of appropriate data for model testing (Wohlfahrt et al., 2001). In the light of these difficulties the correspondence between simulated and measured soil heat fluxes seems acceptable, also because the correction applied to soil heat flux measurements (see Subsection 2.2) shows some variation ($r^2 = 0.80$), which requires further analysis.

With slopes and y-intercepts of linear regressions between measured and simulated air temperatures and vapour pressures between 0.85–0.90 and 0.29–2.53 (°C, hPa; Table III), respectively, predictions by the present model are comparable to other modelling exercises of this kind (Baldocchi, 1992; Gu et al., 1999; Marcolla et al., 2003; Wilson et al., 2003). Some of the high (up to 40 °C) air temperatures measured close to the soil surface must though be viewed with caution, since they might result from the radiation shields being displaced by moving plant parts or thermoelements getting into contact with surrounding phytoelements (Wohlfahrt et al., 2001). Similarly, water vapour pressure measurements in the lower canopy layers may be suspected to be biased towards higher values due to condensation taking place within the tubing (e.g., DOY 189 in Figure 7), which has been argued also by Siqueira et al. (2003). Also measured CO_2 concentrations close to the soil surface are in the need for explanation, since either biologically unsustainable soil respiration rates or extremely high resistances to turbulent diffusion, which would cause simulated temperatures and vapour pressures to exceed measurements by far, would be required to make model simulations match measurements (result of sensitivity tests not shown). One cause for the seemingly unrealistic scalar concentrations close to the soil surface, argued already by Baldocchi (1992), might be that time-averaged scalar concentrations, particularly in the dense canopy region close to the soil surface, are heavily weighted towards long quiescent periods during which scalar material accumulates, before it is flushed out by way of quick sweeps and ejections (Finnigan, 2000). This intermittency may be further exacerbated by stable stratification of the lower canopy layers during times when the upper layers are already unstable. These arguments are supported by the, as compared to the upper canopy layers, generally larger standard deviations of concentration measurements close to the soil surface (Figure 7).

5. Conclusion

Two simple analytical Lagrangian models, the localised near-field theory of Raupach (1989a, b) and the Warland and Thurtell (2000) mixing matrix model, as well as a Lagrangian random walk model of Baldocchi (1992), together with three options for the parameterisation of the Lagrangian time scale, are compared in the present paper in their ability to predict fluxes and scalar concentrations of CO_2, H_2O and sensible heat within and above a mountain meadow canopy. Results indicate that both scalar concentrations and ecosystem fluxes exhibit little sensitivity to the differences between the investigated models and may be predicted satisfactorily by one of the simpler models as long as the source/sink strength is parameterised correctly. Future efforts should thus be directed towards improving other model components (e.g., soil-to-air exchange, phytoelement boundary-layer conductance, radiative transfer), as well as the parameterisation of the source/sink strength (e.g., effects of phenological development, temperature acclimation, disturbance). Model results also show little sensitivity to the parameterisation of the vertical variation of the Lagrangian time scale, yet a unified treatment of the effects of canopy structure on the magnitude and vertical variation of the Lagrangian time scale seems highly desirable. An attempt at this is the second-order closure model by Massman and Weil (1999), yet the larger magnitude and the increase of the Lagrangian time scale towards the ground predicted by their model resulted in less agreement with measurements as compared to the Raupach (1988) and Leuning et al. (2000) parameterisation.

Appendix A: SVAT Model Theory

A.1. Leaf gas exchange

Following theory developed by Farquhar et al. (1980) and Farquhar and Von Caemmerer (1982) CO_2 assimilation is either entirely limited by the kinetic properties of the enzyme RUBISCO (ribulose-1,5-bisphosphate carboxylase/oxygenase) and the respective concentrations of the competing gases CO_2 and O_2 at the sites of carboxylation (W_C, RUBISCO limited rate of carboxylation) or by electron transport (W_J, RuBP limited rate of carboxylation), which limits the rate at which RuBP (ribulose-1,5-bisphosphate) is regenerated. Net photosynthesis A (μmol m^{-2} s^{-1}) may then be expressed as

$$A = \left(1 - \frac{0.5 O_i}{\tau C_i}\right) \min\{W_C, W_J\} - R_{\text{day}}, \tag{A1}$$

where O_i and C_i are the concentrations of O_2 (mmol mol^{-1}) and CO_2 (μmol mol^{-1}) in the intercellular space, respectively. τ is the specificity factor for RUBISCO (–) and R_{day} is the rate of CO_2 evolution from processes other than

photorespiration (μmol m^{-2} s^{-1}). The nitrogen dependencies of the major component processes of A (all in μmol m^{-2} s^{-1}), the maximum rate of carboxylation (V_{Cmax}), the potential rate of RuBP regeneration (P_{ml}) and the dark respiration (R_{dark}), is taken into account using a linear approach described in Wohlfahrt et al. (1998). RUBISCO parameters were taken from Von Caemmerer et al. (1994), with the internal resistance to CO_2 diffusion taken as zero.

To be able to predict gas exchange at the leaf level, the photosynthesis model needs to be linked to a model of stomatal conductance. For this purpose the empirical model by Ball et al. (1987), including the modifications by Falge et al. (1996), was chosen

$$g_{sv} = g_{min} + G_{fac}(A + I_{fac}R_{dark})10^3 \frac{h_s}{C_s}, \tag{A2}$$

where g_{sv} is the stomatal conductance (mmol m^{-2} s^{-1}), g_{min} is the minimum or residual stomatal conductance (mmol m^{-2} s^{-1}) and h_s and C_s are the relative humidity (fraction) and the CO_2 concentration (μmol mol^{-1}) at the leaf surface. G_{fac} is an empirical coefficient representing the composite sensitivity of stomata to these factors and I_{fac} represents the extent to which dark respiration is inhibited in the light.

A.2. THE ENERGY BALANCE

Phytoelement surface temperatures are estimated solving their energy balance equation

$$\begin{aligned} R_{abs} + L_e + LE + H &= 2\epsilon_c \sigma T_{pK}^4 + \frac{\rho c_p}{\gamma}[E_s(T_p) - E_{air}]g_{tv} \\ &\quad + \rho c_p(T_p - T_{air})g_{bh}, \end{aligned} \tag{A3}$$

where R_{abs} is the bi-directional absorbed short-wave and long-wave radiation, L_e is the emitted longwave radiation, LE and H represent latent and sensible heat exchange, respectively (all W m^{-2}); ϵ_c is the phytoelement thermal emissivity, σ is the Stefan–Boltzman constant (5.67×10^{-8} W m^{-2} K^{-4}), ρ and c_p are the density (kg m^{-3}) and the specific heat (1010 J kg^{-1} K^{-1}) of dry air, respectively; γ is the psychrometric constant (Pa K^{-1}), $E_s(T_p)$ is the saturated leaf water vapour pressure (hPa) at the phytoelement temperature T_p (°C), E_{air} the air water vapour pressure (hPa), T_{air} the air temperature (°C), g_{bh} the all-sided phytoelement boundary-layer conductance to heat and g_{tv} the total conductance to water vapour (m s^{-1}). Phytoelement boundary layer conductances are modelled making use of the non-dimensional groups, depending on whether forced or free convection, laminar or turbulent flow prevails (Schuepp, 1993). If phytoelements are wet (either due to dew formation, or the interception of precipitation or dew), g_{tv} is assumed to reduce to g_{bv}, the phytoelement boundary-layer conductance to water vapour.

TABLE A1

Parameters of the combined leaf photosynthesis and stomatal conductance model of the investigated species (Wohlfahrt et al., 1998).

Parameter		Units	CaCa	RaAc	TaOf	TrPr	TrRe	GL	HL
V_{Cmax}	C_N	mmol mol^{-1} s^{-1}	0.851	0.349	0.290	0.381	0.618	0.396	0.459
	C_0	μmol m^{-2} s^{-1}	-15.56	23.76	31.87	32.92	-7.37	35.02	16.72
	ΔH_a	J mol^{-1}	159344	79266	76304	63563	80699	70572	86858
	ΔS	J mol^{-1} K^{-1}	678	663	653	649	660	655	660
P_{ml}	P_{fac}	–	0.564	0.666	0.539	0.592	0.637	0.715	0.598
	ΔH_a	J mol^{-1}	61894	53000	55887	123258	58195	43074	66648
	ΔS	J mol^{-1} K^{-1}	662	655	652	672	656	653	659
R_{dark}	R_{fac}	–	0.021	0.024	0.026	0.028	0.018	0.030	0.023
	ΔH_a	J mol^{-1}	26406	31473	35134	31600	45337	24557	33442
α		mol CO$_2$ mol photons^{-1}	0.055	0.060	0.060	0.060	0.054	0.060	0.058
G_{fac}		–	7.1	14.0	13.0	10.4	9.5	10.2	10.5
g_{min}		mmol m^{-2} s^{-1}	65	45	15	10	30	10	27

Carum carvi (CaCa), *Ranunculus acris* (RaAc), *Taraxacum officinalis* (TaOf), *Trifolium pratensis* (TrPr), *Trifolium repens* (TrRe), graminoid leaves (GL) and herb leaves (HL). C_N and C_0 are the slope and y-intercept, respectively, relating V_{Cmax} at the reference temperature to the leaf nitrogen content (mmol m^{-2}), ΔH_a is the energy of activation, ΔS is an entropy term, P_{fac} and R_{fac} represent the relation between P_{ml} and R_{dark} to V_{Cmax} at the reference temperature, respectively, and α is the apparent quantum yield at saturating CO$_2$. The energy of deactivation, ΔH_d, of V_{Cmax} and P_{ml} were both fixed at 200,000 J mol^{-1}. For other symbols refer to Appendix A.

Dew forms on a phytoelement surface if the surface temperature drops below the dew point temperature of the surrounding air. The calculations of dew dynamics recognise that phytoelements hold water up to a maximum capacity before the onset of dripping to the canopy components below, following an approach described in Wilson et al. (1999). Interception of precipitation is taken into account following Watanabe and Mizutani (1996). The energy balance algorithm is solved in an analytical fashion following Nikolov et al. (1995).

A.3. MOMENTUM TRANSFER AND VERTICAL VELOCITY STANDARD DEVIATION

Momentum transfer by the vegetation cover is simulated using the model by Massman (1997), which predicts the mean horizontal wind speed and the shear stress within the canopy as a function of the PAD ($m^2\ m^{-3}$) and an effective phytoelement drag coefficient. The latter is parameterised as a function of PAD, as proposed and tested by Wohlfahrt and Cernusca (2001) for this meadow. The decrease of the vertical velocity standard deviation (σ_w) with canopy depth is modelled after Massman and Weil (1999).

A.4. RADIATIVE TRANSFER

Radiative transfer is simulated following the basic theory developed by Goudriaan (1977), modified to accommodate multiple species and components (Wohlfahrt et al., 2001). The model treats the canopy as a horizontally homogeneous, plane-parallel turbid medium in which multiple scattering occurs on the elements of turbidity (phytoelements) of the different components, each having their own optical and geometrical properties. The canopy is divided into sufficiently small (0.1 $m^2\ m^{-2}$), statistically independent layers, within which self-shading may be considered negligible and phytoelements to be distributed symmetrically with respect to the azimuth. Hemispherical reflection and transmission of radiation, which are allowed to be unequal, are assumed to be lambertian. The model accounts for the bi-modal distribution of solar radiation within the canopy, sunlit phytoelements receiving both direct and diffuse radiation, while shaded ones receive diffuse radiation only. Phytoelement and soil optical properties were taken from various literature sources as described in Wohlfahrt et al. (2001). Solar elevation is calculated using the equations given in Campbell and Norman (1998). Partitioning of solar radiation into direct and diffuse PPFD and near infrared components is modelled using the approach described in Gu et al. (2002).

A.5. SOIL HEAT AND WATER FLUX

The soil heat flux (q_h, W m^{-2}) is modelled as the sum of heat conduction and convection as

$$q_h = -k_h \frac{\delta T}{\delta z} + C_w T q_w + \lambda q_v, \tag{A4}$$

where q_w is the flux of liquid water (kg m^{-2} s^{-1}), q_v is the vapour flux (kg m^{-2} s^{-1}), k_h is the thermal conductivity (W m^{-1} K^{-1}), T is the temperature (K), C_w is the specific heat of liquid water (J kg^{-1} K^{-1}), λ is the latent heat of vaporisation (J kg^{-1}) and z is depth (m). The soil surface energy balance is solved in an analytical fashion using a modification to the approach of Nikolov et al. (1995).

Water flow in the soil is assumed to be laminar and thus to obey Darcy's law as generalised for unsaturated flow,

$$q_w = -k_w(\theta) \left(\frac{\delta \psi(\theta)}{\partial z} - 1 \right) + D_v \frac{\delta C_v}{\delta z}, \tag{A5}$$

where ψ is the matric potential (J kg^{-1}), k_w is the hydraulic conductivity (kg s m^{-3}), C_v the vapour concentration in soil air (kg m^{-3}), D_v the diffusion coefficient for water vapour in the soil (m^2 s^{-1}), and θ the volumetric water content (m^3 m^{-3}). Soil evaporation is modelled following Baldocchi et al. (2000). Both soil heat and water fluxes are solved numerically using a 10-layer model as described in Campbell (1985).

References

Aubinet, M., Grelle, A., Ibrom, A., Rannik, Ü., Moncrieff, J., Foken, T., Kowalski, A. S., Martin, P. H., Berbigier, P., Bernhofer, Ch., Clement, R., Elbers, J., Granier, A., Grünwarld, T., Morgenstern, K., Pilegaard, K., Rebmann, C., Snijders, W., Valentini, R., and Vesala, T.: 2000, 'Estimates of the Annual Net Carbon and Water Exchange of Forest: The EUROFLUX Methodology', *Adv. Ecol. Res.* **30**, 113–175.

Baldocchi, D. D.: 1992, 'A Lagrangian Random Walk Model for Simulating Water Vapor, CO_2 and Sensible Heat Flux Densities and Scalar Profiles over and within a Soybean Canopy', *Boundary-Layer Meteorol.* **61**, 113–144.

Baldocchi, D. D.: 1993, 'Scaling Water Vapour and Carbon Dioxide Exchange from Leaves to a Canopy: Rules and Tools', in J. R. Ehleringer and C. B. Field (eds.), *Scaling Physiological Processes*, Academic Press, San Diego, pp. 77–114.

Baldocchi, D. D.: 2003, 'Assessing the Eddy Covariance Technique for Evaluating Carbon Dioxide Exchange Rates of Ecosystems: Past, Present and Future', *Global Change Biol.* **9**, 479–492.

Baldocchi, D. D. and Harley, P. C.: 1995, 'Scaling Carbon Dioxide and Water Vapour Exchange from Leaf to Canopy in a Deciduous Forest. II. Model Testing and Application', *Plant Cell Environ.* **18**, 1157–1173.

Baldocchi, D. D. and Meyers, T.: 1998, 'On Using Eco-Physiological, Micrometeorological and Biogeochemical Theory to Evacuate Carbon Dioxide, Water Vapour and Trace Gas Fluxes over Vegetation: A Perspective', *Agric. For. Meteorol.* **90**, 1–25.

Baldocchi, D. D. and Wilson, K. B.: 2001, 'Modelling CO_2 and Water Vapour Exchange of a Temperate Broadleaved Forest across Hourly to Decadal Time Scales', *Ecol. Model.* **142**, 155–184.

Baldocchi, D. D., Hicks, B. B., and Meyers, T. P.: 1988, 'Measuring Biosphere-Atmosphere Exchanges of Biologically Related Gases with Micrometeorological Methods', *Ecology* **69**, 1331-1340.

Baldocchi, D. D., Law, B. E., and Anthoni, P. M.: 2000, 'On Measuring and Modelling Energy Fluxes above the Floor of a Homogeneous Conifer Forest', *Agric. For. Meteorol.* **102**, 187–206.

Ball, J. T., Woodrow, I. E., and Berry, J. A.: 1987, 'A Model Predicting Stomatal Conductance and its Contribution to the Control of Photosynthesis under Different Environmental Conditions', in J. Biggens (ed.), *Progress in Photosynthesis Research Vol. IV*, *Proceedings of the VII International Congress on Photosynthesis*, Martinus Nijhoff, Dordrecht, pp. 221–224.

Campbell, G. S.: 1985, *Soil Physics with BASIC*, Elsevier, Amsterdam, 150 pp.

Campbell, G. S. and Norman, J. M.: 1998, *An Introduction to Environmental Biophysics*, Springer Verlag, New York, 286 pp.

Cernusca, A. and Decker, P.: 1989, 'Faktorenabhängigkeit der Respiratorischen Kohlenstoffverluste einer Alpinen Grasheide (Caricetum curvulae) in 2300 m MH in den Hohen Tauern', in A. Cernusca (ed.), *Struktur und Funktion von Graslandökosystemen im Nationalpark Hohe Tauern, Veröffentlichungen des österreichischen MaB-Programms*, Band 13, Universitätsverlag Wagner, Innsbruck, pp. 371–396.

Davidson, E. A., Savage, K., Verchot, L. V., and Navarro, R.: 2002, 'Minimizing Artifacts and Biases in Chamber-Based Measurements of Soil Respiration', *Agric. For. Meteorol.* **113**, 21–37.

Denmead, O. T., Harper, L. A., and Sharpe, R. R.: 2000, 'Identifying Sources and Sinks of Scalars in Corn Canopy with Inverse Lagrangian Dispersion Analysis. I. Heat', *Agric. For. Meteorol.* **104**, 67–73.

Dolman, A. J. and Wallace, J. S.: 1991, 'Lagrangian and K-Theory Approaches in Modelling Evaporation from Sparse Canopies', *Quart. J. Roy. Meteorol. Soc.* **117**, 1325–1340.

Falge, E., Graber, W., Siegwolf, R., and Tenhunen, J. D.: 1996, 'A Model of the Gas Exchange of *Picea abies* to Habitat Conditions', *Trees* **10**, 277–287.

Farquhar, G. D. and Von Caemmerer, S.: 1982, 'Modelling of Photosynthetic Response to Environmental Conditions', in O. L. Lange, P. S. Nobel, C. B. Osmond, and H. Ziegler (eds.), *Physiological Plant Ecology Vol. II, Encyclopaedia of Plant Physiology 12B*, Springer Verlag, Berlin, pp. 549–588.

Farquhar, G. D., Von Caemmerer, S., and Berry, J. A.: 1980, 'A Biochemical Model of Photosynthetic CO_2 Assimilation in Leaves of C3 Species', *Planta* **149**, 78–90.

Finnigan, J. J.: 2000, 'Turbulence in Plant Canopies', *Annu. Rev. Fluid Mech.* **32**, 519–571.

Foken, T. and Wichura, B.: 1996, 'Tools for Quality Assessment of Surface-Based Flux Measurements', *Agric. For. Meteorol.* **78**, 83–105.

Gilman, K.: 1977, *Movement of Heat in Soils*, Institute of Hydrology Report no. 44, Institute of Hydrology, Wallingford, Oxon, 45 pp.

Goudriaan, J.: 1977, *Crop Micrometeorology: A Simulation Study*, Pudoc, Wageningen, 249 pp.

Goulden, M. L., Munger, J. W., Fan, S.-M., Daube, B. C., and Wofsy, S. C.: 1996, 'Measurements of Carbon Sequestration by Long-Term Eddy Covariance: Methods and Critical Evaluation of Accuracy', *Global Change Biol.* **2**, 169–182.

Gu, L., Baldocchi, D. D., Verma, S. B., Black, T. A., Vesala, T., Falge, E. M., and Dowty, P. R.: 2002, 'Superiority of Diffuse Radiation for Terrestrial Ecosystem Productivity', *J. Geophys. Res.* **107**, DOI 10.1029/2001/JD001242.

Gu, L., Shugart, H. H., Fuentes, J. D., Black, T. A., and Shewchuk, S. R.: 1999, 'Micrometeorology, Biophysical Exchanges and NEE Decomposition in a Two-Story Boreal Forest – Development and Test of an Integrated Model', *Agric. For. Meteorol.* **94**, 123–148.

Harper, L. A., Denmead, O. T., and Sharpe, R. R.: 2000, 'Identifying Sources and Sinks of Scalars in a Corn Canopy with Inverse Lagrangian Dispersion Analysis. II. Ammonia', *Agric. For. Meteorol.* **104**, 75–83.

Jarvis, P. G., Massheder, J. M., Hale, S. E., Moncrieff, J. B., Rayment, M., and Scott, S. L.: 1997, 'Seasonal Variation of Carbon Dioxide, Water Vapour and Energy Exchanges of a Boreal Black Spruce Forest', *J. Geophys. Res.* **102**, 28953-28966.

Kaimal, J. C. and Finnigan, J. J.: 1994, *Atmospheric Boundary Layer Flows*, Oxford University Press, Oxford, 289 pp.

Katul, G., Oren, R., Ellsworth, D., Hsieh, C.-I., and Philipps, N.: 1997, 'A Lagrangian Dispersion Model for Predicting CO_2 Sources, Sinks, and Fluxes in a Uniform Loblolly Pine (*Pinus taeda* L.) Stand', *J. Geophys. Res.* **102**, 9309–9321.

Lai, C.-T., Katul, G., Butnor, J., Ellsworth, D., and Oren, R.: 2002a, 'Modelling Night-Time Ecosystem Respiration by a Constrained Source Optimization Method', *Global Change Biol.* **8**, 124–141.

Lai, C.-T., Katul, G., Butnor, J., Siqueira, M., Ellsworth, D., Maier, C., Johnsen, K., McKeand, S., and Oren, R.: 2002b, 'Modelling the Limits on the Response of Net carbon Exchange to Fertilization in a South-East Pine Forest', *Plant Cell Environ.* **25**, 1095–1119.

Lai, C.-T., Katul, G., Ellsworth, D., and Oren, R.: 2000a, 'Modelling Vegetation-Atmosphere CO_2 Exchange by a Coupled Eulerian–Lagrangian Approach', *Boundary-Layer Meteorol.* **95**, 91–122.

Lai, C.-T., Katul, G., Oren, R., Ellsworth, D., and Schäfer, K.: 2000b, 'Modelling CO_2 and Water Vapour Turbulent Flux Distribution within a Forest Canopy', *J. Geophys. Res.* **105**, 2633–26351.

Larcher, W.: 2001, *Ökophysiologie der Pflanzen*, Verlag Eugen Ulmer, Stuttgart, 408 pp.

Legg, B. J. and Raupach, M. R.: 1982, 'Markov–Chain simulation of Particle Dispersion in Inhomogeneous Flows: The Mean Drift Velocity Induced by the Gradient in Eulerian Velocity Variance', *Boundary-Layer Meteorol.* **24**, 3–13.

Leuning, R.: 2000, 'Estimation of Scalar Source/Sink Distributions in Plant Canopies Using Lagrangian Dispersion Analysis: Corrections for Atmospheric Stability and Comparison with a Multilayer Canopy Model', *Boundary-Layer Meteorol.* **96**, 293–314.

Leuning, R., Denmead, O. T., Miyata, A., and Kim, J.: 2000, 'Source/Sink Distributions of Heat, Water Vapour, Carbon Dioxide and Methane in a Rice Canopy Estimated Using Lagrangian Dispersion Analysis', *Agric. For. Meteorol.* **104**, 233–249.

Mahfouf, J. F. and Noilhan, J.: 1991, 'Comparative Study of Various Formulations of Evaporation from Bare Soil Using *in situ* Data', *J. Appl. Meteorol.* **30**, 1354–1365.

Marcolla, B., Pitacco, A., and Cescatti, A.: 2003, 'Canopy Architecture and Turbulence Structure in a Coniferous Forest', *Boundary-Layer Meteorol.* **108**, 35–59.

Massman, W. J.: 1997, 'An Analytical One-Dimensional Model of Momentum Transfer by Vegetation of Arbitrary Structure', *Boundary-Layer Meteorol.* **83**, 407–421.

Massman, W. J. and Weil, J. C.: 1999, 'An Analytical One-Dimensional Second-Order Closure Model of Turbulence Statistics and the Lagrangian Time Scale within and above Plant Canopies of Arbitrary Structure', *Boundary-Layer Meteorol.* **91**, 81–107.

McMillen, R. T.: 1988, 'An Eddy Correlation System with Extended Applicability to Non-Simple Terrain', *Boundary-Layer Meteorol.* **43**, 231–245.

McNaughton K. G. and Van den Hurk B. J. J. M.: 1995, 'A Lagrangian Revision of the Resistors in the Two Layer Model for Calculating the Energy Budget of a Plant Canopy', *Boundary-Layer Meteorol.* **74**, 261–288.

Monsi, M. and Saeki, T.: 1953, 'Über den Lichtfaktor in den Pflanzengesellschaften und seine Bedeutung für die Stoffproduktion', *Jap. J. Bot.* **14**, 22–52.

Moore, C. J.: 1986, 'Frequency Response Corrections for Eddy Correlation Systems', *Boundary-Layer Meteorol.* **37**, 17–35.

Nikolov, N. T and Zeller, K. F.: 2003, 'Modelling Coupled Interactions of Carbon, Water, and Ozone Exchange between Terrestrial Ecosystems and the Atmosphere. I: Model Description', *Environ. Poll.* **124**, 231–246.

Nikolov, N. T., Massman, W. J., and Schoettle, A. W.: 1995, 'Coupling Biochemical and Biophysical Processes at the Leaf Level: An Equilibrium Photosynthesis Model for Leaves of C_3 Plants', *Ecol. Model.* **80**, 205–235.

Ogee, J. and Brunet, Y.: 2002, 'A Forest Floor Model for Heat and Moisture Including a Litter Layer', *J. Hydrol.* **255**, 212–233.

Ogee, J., Brunet, Y., Loustau, D., Berbigier, P., and Delzon, S.: 2003, 'MuSICA, a CO_2, Water and Energy Multilayer, Multileaf Pine Forest Model: Evaluation from Hourly to Yearly Time Scales and Sensitivity Analysis', *Global Change Biol.* **9**, 697–717.

Raupach, M. R.: 1987, 'A Lagrangian Analysis of Scalar Transfer in Vegetation Canopies', *Quart. J. Roy. Meteorol. Soc.* **113**, 107–120.

Raupach, M. R.: 1988, 'Canopy Transport Processes', in W. L. Steffen and O. T. Denmead (eds.), *Flow and Transport in the Natural Environment*, Springer Verlag, Berlin, pp. 95–127.

Raupach, M. R.: 1989a, 'A Practical Lagrangian Method for Relating Scalar Concentrations to Source Distributions in Vegetation Canopies', *Quart. J. Roy. Meteorol. Soc.* **115**, 609–632.

Raupach, M. R.: 1989b, 'Applying Lagrangian Fluid Mechanics to Infer Scalar Source Distributions from Concentration Profiles in Plant Canopies', *Agric. For. Meteorol.* **47**, 85–108.

Raupach, M. R., Finkele, K., and Zhang, L.: 1997, *SCAM (Soil-Canopy-Atmosphere Model) Description and Comparison with Field Data*, CSIRO, Centre for Environmental Mechanics, Technical Report No. 132, Canberra, 81 pp.

Raupach, M. R., Finnigan, J. J., and Brunet, Y.: 1996, 'Coherent Eddies and Turbulence in Vegetation Canopies: The Mixing-Layer Analogy', *Boundary-Layer Meteorol.* **78**, 351–382.

Rayment, M. B.: 2000, 'Closed Chamber Systems Underestimate Coil CO_2 Efflux', *Eur. J. Soil Sci.* **51**, 107–110.

Ross, J.: 1981, *The Radiation Regime and Architecture of Plant Stands*, Junk Publishers, The Hague, 391 pp.

Schotanus, P., Nieuwstadt, F. T. M., and de Bruin, H. A. R.: 1983, 'Temperature Measurement with a Sonic Anemometer and Its Application to Heat and Moisture Flux', *Boundary-Layer Meteorol.* **26**, 81–93.

Schuepp, P. H.: 1993, 'Tansley Review No. 59: Leaf Boundary Layers', *New Phytologist* **125**, 477–507.

Siqueira, M., Katul, G., and Lai, C.-T.: 2002, 'Quantifying Net Ecosystem Exchange by Multilevel Ecophysiological and Turbulent Transport Models', *Adv. Water Res.* **25**, 1357–1366.

Siqueira, M., Leuning, R., Kolle, O., Kelliher, F.M., and Katul, G.G.: 2003, 'Modelling Sources and Sinks of CO_2, H_2O and Heat within a Siberian Pine Forest Using Three Inverse Methods', *Quart. J. Royal Meteorol. Soc.* **129**, 1373–1393.

Tappeiner, U. and Cernusca, A.: 1998, 'Model Simulation of Spatial Distribution of Photosynthesis in Structurally Differing Plant Communities in the Central Caucasus', *Ecol. Model.* **113**, 201–223.

Tappeiner, U., Cernusca, A., Siegwolf, R. T. W., Sapinsky, S., Newesely, Ch., Geissbühler, P., and Stefanicki, G.: 1999, 'Microclimate, Energy Budget and CO_2 Gas Exchange of Ecosystems', in A. Cernusca, U. Tappeiner, and N. Bayfield (eds.), *Land-Use Changes in European Mountain Ecosystems. ECOMONT – Concepts and Results*, Blackwell Wissenschafts-Verlag, Berlin, pp. 135–145.

Thomson, D. J.: 1987, 'Criteria for the Selection of Stochastic Models for Particle Trajectories in Turbulent Flows', *J. Fluid Mech.* **180**, 529–556.

Van den Hurk, B. J. J. M. and McNaughton, K. G.: 1995, 'Implementation of Near-Field Resistance in a Simple Two-Layer Surface Resistance Model', *J. Hydrol.* **166**, 293–311.

Von Caemmerer, S., Evans, J. R., Hudson, G. S., and Andrews, T. J.: 1994, 'The Kinetics of Ribulose-1,5-Bisphosphate Carboxylase/Oxygenase in vivo Inferred from Measurements of Photosynthesis in Leaves of Transgenic Tobacco', *Planta* **195**, 88–97.

Warland, J. S. and Thurtell, G. W.: 2000, 'A Lagrangian Solution to the Relationship between a Distributed Source and Concentration Profile', *Boundary-Layer Meteorol.* **96**, 453–471.

Watanabe, T. and Mizutani, K.: 1996, 'Model Study on the Micrometeorological Aspects of Rainfall Interception Over an Evergreen Broad-Leaved Forest', *Agric. For. Meteorol.* **80**, 195–214.

Williams, M., Rastetter, E. B., Fernandes, D. N., Goulden, M. L., Wofsy, S. C., Shaver, G. R., Melillo, J. M., Munger, J. W., Fan, S.-M., and Nadelhoffer K. J.: 1996, 'Modelling the Soil-Plant-Atmosphere Continuum in a Quercus-Acer Stand at Harvard Forest: The Regulation of Stomatal Conductance by Light, Nitrogen and Soil/Plant Hydraulic Properties', *Plant Cell Environ.* **19**, 911–927.

Wilson, T. B., Bland, W. L., and Norman J. M.: 1999, 'Measurement and Simulation of Dew Accumulation and Drying in a Potato Canopy', *Agric. For. Meteorol.* **93**, 111–119.

Wilson, T. B., Norman, J. M., Bland, W. L., and Kucharik, C. J.: 2003, 'Evaluation of the Importance of Lagrangian Canopy Turbulence Formulations in a Soil-Plant-Atmosphere Model', *Agric. For. Meteorol.* **115**, 51–69.

Wohlfahrt, G. and Cernusca, A.: 2001, 'Momentum Transfer by a Mountain Meadow Canopy: A Simulation Analysis Based on Massman's (1997) Model', *Boundary-Layer Meteorol.* **103**, 391–407.

Wohlfahrt, G., Bahn, M., Haubner, E., Horak, I., Michaeler, W., Rottmar, K., Tappeiner, U., and Cernusca, A.: 1999, 'Inter-Specific Variation of the Biochemical Limitation to Photosynthesis and Related Leaf Traits of 30 Species from Mountain Grassland Ecosystems under Different Land Use', *Plant Cell Environ.* **22**, 1281–1296.

Wohlfahrt, G., Bahn, M., Horak, I., Tappeiner, U., and Cernusca, A.: 1998, 'A Nitrogen Sensitive Model of Leaf Carbon Dioxide and Water Vapour Gas Exchange: Application to 13 Key Species from Differently Managed Mountain Grassland Ecosystems', *Ecol. Model.* **113**, 179–199.

Wohlfahrt, G., Bahn, M., Tappeiner, U., and Cernusca, A.: 2000, 'A Model of Whole Plant Gas Exchange for Herbaceous Species from Mountain Grassland Sites Differing in Land Use', *Ecol. Model.* **125**, 173–201.

Wohlfahrt, G., Bahn, M., Tappeiner, U., and Cernusca, A.: 2001, 'A Multi-Component, Multi-Species
    Model of Vegetation-Atmosphere CO_2 and Energy Exchange for Mountain Grasslands', *Agric.
    For. Meteorol.* **106**, 261–287.